Diploma thesis

RNA interference in HepG2 cells to investigate the role of BCS1L in respiratory chain function

Submitted by

Veronika Marlies Berghold

Mat.Nr.: 0312256

In partial fulfilment of the requirements for the degree of

Doctor of Medicine

at the

Medical University of Graz

carried out at the

Department of Clinical Sciences, Division of Peadiatrics, Biomedical Center, Lund University, Sweden

Supervisors

Professor Vineta Fellman, MD, PhD,
Associate Professor Per Levéen, PhD
Department of Clinical Sciences, Division of Paediatrics,
Lund University

Ao.Univ.-Prof. Dr. Barbara Plecko-Startinig
Department of Paediatrics and Adolesence Medicine,
Medical University of Graz

Affidavit

I hereby declare that the following master thesis has been written only by the undersigned and without any assistance from third parties. Furthermore, I confirm that no sources have been used in the preparation of this thesis other than those indicated in the thesis itself. I clearly marked content or ideas borrowed from other sources as not my own and documented their sources.

Graz, September 2010 *Signature*

Preface

During my Erasmus exchange student year in 2007/2008 at the Lund University, Sweden I had the great opportunity to join the group of Professor Vineta Fellman at the Biomedical Center (BMC C14). For a few years I wanted to become a paediatrician and was excited about the chance to work in a research group of that field.

In 1998 Vineta Fellman described the GRACILE syndrome (growth retardation, aminoaciduria, cholestasis, iron overload, lactic acidosis and early death) as a new disease entity. Following, in 2002 the underlying homozygous mutation in the *BCS1L* gene was identified. *BCS1L* encodes a mitochondrial protein which is responsible for the proper incorporation of the Rieske iron-sulfur protein subunit into complex III of the respiratory chain.

The aim of my project was to create a cell model of human liver carcinoma cells. We wanted to study the effects on cells missing the gene. During my eight month project I learned some fundamental methods of basic research and laboratory work including cell line cultivation, siRNA transfections, mRNA and protein analyses. I thoroughly enjoyed working in the lab and discovered my enthusiasm about fundamental research. After earning my degree I further plan to work in research.

In the introduction of my thesis I start with giving an overall view of the physiology of mitochondria with a special emphasis on the respiratory chain. I continue with a more detailed description of complex III and *BCS1L*.

The second part talks about mitochondrial diseases in general and further covers the three main clinical phenotypes caused by *BCS1L* mutations which are the GRACILE syndrome, Complex III deficiencies and the Björnstad syndrome.

The last chapter of the introduction describes the theoretical background of the cell model, in particular RNA interference.

In materials and methods I describe all the methods I learned and used throughout the project. I present our results and discuss them in the conclusion.

Acknowledgement

First of all, I want to sincerely thank Professor Vineta Fellman, PhD, MD, Professor of Neonatology, University of Lund, Sweden who offered me the opportunity to work in her laboratory. She introduced me to the project and all her co-workers. Although her time was limited she always wanted to be informed about the progress and gave new ideas. I am very grateful to Professor Fellman to prolong and fund my stay for further two months which let me finish my experimental series.

My deepest gratitude goes to Associate Professor Per Levéen, PhD who was my supervisor throughout the project. He taught me about culturing cells, RNA interference and also gave me insights in different aspects of research. Professor Levéen was very patient answering all my questions while he gave me the chance to plan and conduct experiments on my own.

In particular, I want to thank Heike Kotarsky, PhD who taught me about Western Blot, BNP and Immunofluoresence and gave me steady support. Furthermore I want to thank Eva Hansson for her technical advice and Associate Professor Eskil Elmér, MD, PhD for the introduction to high resolution respirometry.

Deep appreciation goes to Ao.Univ.-Prof. Dr. Barbara Plecko-Startinig from the Medical University of Graz who encouraged me to take the possibility to do my thesis abroad and gave valuable input on the project.

Last but not least I want to thank my family and friends for their support and understanding.

Abstract

Background and Aims: The human *BCS1L* gene encodes a mitochondrial protein which functions as a chaperone for the incorporation of the subunit Rieske iron-sulfur protein (RISP) into complex III of the mitochondrial respiratory chain.
Mutations in *BCS1L* result in several mitochondrial disorders of various severities such as the GRACILE syndrome, Complex III deficiencies and the Björnstad syndrome. The GRACILE syndrome (Fellmans syndrome, MIM #603358) is characterized by fetal growth retardation, aminoaciduria due to tubulopathy, cholestasis, iron overload, lactacidosis, and early death. Complex III deficiency (MIM #124000) causes encephalopathy with or without visceral involvement. The Björnstad syndrome (MIM #262000) manifests as congenital hearing loss and pili torti, however, is compatible with normal adult life.
To further investigate the functional role of BCS1L we silenced the *BCS1L* gene using RNA interference in HepG2 cells of a hepatocarcinoma cell line.

Methods: In order to downregulate the expression of *BCS1L*, HepG2 cells were transfected with small interfering RNAs (siRNAs) directed against *BCS1L* mRNA. This leads to degradation of mRNA and thus prevents the expression of the BCS1L protein. In order to achieve maximum decrease of RISP incorporation, transfections were repeated three times with a two-day interval.
RNA was prepared from BCS1L deficient and control HepG2 cells. Subsequently, cDNA synthesis and real-time PCR were preformed to determine the expression rate of the *BCS1L* mRNA.
SDS PAGE and Western Blot was used to visualize the downregulation at the protein level. Incorporation of RISP in complex III was studied with Blue Native PAGE.
To study effects on the respiratory chain, cells where analyzed in “high resolution respirometer” (Oroboros O2k Oxygraph). The amount of mitochondria in HepG2 cells was investigated using immunofluorescence with antibodies against pyruvate dehydrogenase and subunit Core1 of complex III.

Results: The expression of *BCS1L* in HepG2 cells was reduced by 80-90% compared to control cells. In agreement with this, Blue Native PAGE showed a significant reduction of RISP amount in complex III after six days of treatment. However, we did not detect any significant changes in mitochondrial respiration compared to control cells. The number of mitochondria was similar in both groups.

Conclusion: The study design resulted in a sufficient downregulation of the target protein to cause a functional deficit, i.e. abnormal assembly of complex III. Surprisingly, mitochondrial respiration *in vitro* was functional despite this complex III abnormality. We therefore postulate that 20% of normal *BCS1L* expression is sufficient to maintain normal cell respiration.

Zusammenfassung

Hintergrund und Fragestellung: Das humane *BCS1L* Gen codiert ein mitochondirales Protein, dessen Aufgabe als Chaperon der Einbau der Untereinheit Rieske Eisen-Schwefel Protein (RISP) in den Komplex III der Atmungskette ist.
Mutationen des *BCS1L* führen zu unterschiedlich schwerwiegenden Mitochondriopathien wie das GRACILE Syndrom, Komplex III Defizienz und das Björnstad Syndrom. Das GRACILE Syndrom (Fellmans Syndrom, MIM #603358) ist charakterisiert durch Wachstumsretardierung, Aminoazidurie aufgrund von Tubulopathie, Cholestase, Eisenüberladung, Laktatazidose und frühem Tod. Komplex III Defizienz (MIM #124000) verursacht Enzephalopathie mit oder ohne viszeraler Beteiligung. Das Björnstad Syndrom (MIM #262000), welches mit angeborenen Gehörverlust und Pili torti manifestiert, ist mit dem Leben vereinbar.
Zur Untersuchung der Funktion von BCS1L wurde das *BCS1L* Gen mittels RNA Interferenz in HepG2 Zellen, eine aus einem Leberzellkarzinom gewonnene Zelllinie, unterdrückt.

Methoden: Um die Expression von *BCS1L* zu vermindern wurden die HepG2 Zellen mit „small interfering RNAs" (siRNAs) transfektiert, welche gegen die *BCS1L* mRNA gerichtet waren. Dies führt zum Abbau von mRNA und in weiterer Folge verhindert es die Expression des BCS1L Proteins. Um die maximale Reduktion des Einbaus von RISP zu erzielen, wurden die Transfektionen 3-mal in 2 Tages Abständen wiederholt.
RNA wurde von BCS1L defizienten HepG2 Zellen und Kontrollen präpariert. Anschließend wurden cDNA synthetisiert und real-time PCR durchgeführt, um die Expressionsrate von *BCS1L* mRNA zu eruieren.
Die verminderte Proteinexpression wurde mit SDS PAGE und Western Blot visualisiert. Der Einbau der RISP Untereinheit in den Komplex III wurde mit Blue Native PAGE untersucht.
Die Zellen wurden im "high resolution respirometer" (Oroboros O2k Oxygraph) analysiert um die mitochondriale Atmungskettenaktivität zu bestimmen. Die Anzahl der Mitochondrien innerhalb der HepG2 Zellen wurde mittels Immunfluoreszenz

untersucht. Die verwendeten Antikörper waren gegen Pyruvatdehydrogenase und Core1, eine weitere Untereinheit von Komplex III, gerichtet.

Ergebnisse: Die Expression von *BCS1L* in HepG2 Zellen war im Vergleich zu den Kontrollzellen um 80-90% vermindert. Übereinstimmend mit diesen Ergebnissen zeigte Blue Native PAGE eine auffällige Verminderung von eingebautem RISP in Komplex III nach 6 Versuchstagen.
Im Gegensatz dazu war es nicht möglich signifikante Veränderungen in der Atmungskettenfunktion im Vergleich zu unbehandelten Zellen festzustellen. Die Anzahl der Mitochondrien war in beiden Gruppen gleich groß.

Schlussfolgerung: Das Untersuchungsdesign ermöglichte eine ausreichende Verminderung des Zielproteins um ein funktionelles Defizit zu verursachen, d.h. die abnormale Aggregation von Komplex III. Überraschenderweise funktionierte jedoch die mitochondoriale Atmung *in vitro* trotz der Komplex III Abnormalität. Aus diesem Grund postulieren wir, dass 20% der normalen *BCS1L* Expression ausreicht um eine suffiziente Atmungskettenfunktion aufrecht zu erhalten.

Table of Contents

List of Abbreviations

acetyl-CoA	acetyl coenzyme A
ACTB	beta actin
ADP	adenosine diphosphate
AGO	Argonaute protein
Ama	Antimycin A
ANC	adenine nucleotides carriers
APS	Ammoniumpersulfat
ATP	adenosine triphosphate
Bcs1	BCS1 gene (yeast)
BCS1L	BCS1-like gene (human)
BCS1L	BCS1-like protein (human)
Bcs1p	Bcs1 protein (yeast)
BNP	Blue Native PAGE
bp	base pairs
Ca^{2+}	calcium
cDNA	complementary DNA
CFNS	Craniofrontonasal syndrome
CO_2	carbondioxide
Core1	complex III subunit Core1
COX	cytochrome c oxidase
CPT-I & II	carnitine palmitoyl transferase I & II
C_t	cycle threshold (real time PCR)
DCR	Dicer
DUF283	Domain of Unknown Function 283
DNA	deoxyribonucleic acid
dNTP	desoxyribonucleoside triphosphate
dsRBD	dsRNA binding domain
dsRNA	double-stranded RNA
dUTP	deoxyuridine triphosphate
ECL	Enhanced Chemiluminescence
EDTA	ethylene-diamine-tetraacetic acid

EFMR	Epilepsy and mental retardation limited to females
FA	fatty acid
FAD	flavin adenine dinucleotide
FBS	fetal bovine serum
FCCP	Carbonyl cyanide p-(trifluoromethoxy) phenylhydrazone
FDH	Finish Disease Heritage
Fe	iron
FITC	fluorescein isothiocyanate
g	gravitational force
GSH	glutathione (L-γ-glutamyl-L-cysteinylglycine)
H_2O	water
HepG2	human hepatoblastoma cell line
HIF-1	hypoxia-inducible factor 1
HiPerFect	HiPerFect Transfection Reagent from Qiagen®
HRP	horse radish peroxidase
ICD 10	International Statistical Classification of Diseases and Related Health Problems, 10th Revision
IgG1	Immunglobulin G1
KCl	potassium chloride
LM	lauryl malthoside (n-Dodecyl-β-n-malthoside)
mM	mili mole
MB2	buffer
Mg^{++}	magnesium
$MgCl_2$	magnesium chloride
mETC	mitochondrial electron transport chain
mM	milli mole
Mn^{++}	mangan
mRNA	messenger RNA
miRNA	microRNA
mtDNA	mitochondrial DNA
Na^+	sodium
NaCl	sodium chloride
NAD^+	nicotinamide adenine dinucleotide

nDNA	nuclear DNA
NGS	normal goat serum
NTC	no template control
O_2	oxygen
MIM	Mendelian Inheritance in Man
Omy	oligomycin
PAGE	polyacrylamide gel electrophoresis
PAZ	Piwi/Argonaute/Zwille domain
PBS	phosphate buffered saline
PBST	phosphate-buffered saline Tween
PCR	polymerase chain reaction
PDH E1	pyruvate dehydrogenase subunit E1
PEEK	polyetheretherketone
PHD	prolyl hydroxylate enzymes
P_i	inorganic phosphate
piRNA	PIWI-interacting RNA
PLP	proteolipid protein
PMD	Pelizaeus–Merzbacher disease
pmf	protein motife force
POS	Polarographic O_2 sensor
PS	Penicillin/Streptomycin
PVDF	polyvinylidene fluoride
Q	Ubiquinone
QH_2	Ubiquinol
Q_i	quinol reductase, also Q_N for negatively charged
Q_o	quinol oxidase, also Q_P for positively charged
RCR	respiratory control ratio
RISC	RNA induced silencing complex
RISP	Rieske iron-sulfur protein
RLC	RISC loading complex
RLT	lysis buffer for purification of total RNA
RNA	ribonucleic acid
RNAi	RNA interference

ROS	reactive oxygen species
Rot	rotenone
RPE	buffer for purification of total RNA
rpm	revolutions per minute
rRNA	ribosomal RNA
RW1	buffer for purification of total RNA
SBG	Serva Blue G
SD	standard deviation
SDS	sodium dodecylsulfate
siRNA	small interfering RNA, small inhibitory RNA, short interfering RNA
SQ	Semiquinone
TBE	Tris/Borate/EDTA buffer
TCA	tricarboxylic acid cycle
Temed	Tetramethylethylenediamine
TfR2	Transferrin receptor 2
tk	thymidine kinase
Tris	tris[hydroxymethyl]aminomethane
tRNA	transfer RNA
UNG	uracil N-glycosylase
UTR	untranslated region

Index of Figures

1. Aims of the study

1) Achieve knockdown of BCS1L mRNA and protein expression in HepG2 cells using RNA interference.
2) Achieve knockdown of Rieske iron-sulfur protein (RISP) mRNA and protein expression in HepG2 cells using RNA interference.
3) Achieve reduced incorporation of RISP into complex III using *BCS1L* and *RISP* siRNA, respectively.
4) Investigate mitochondrial respiration in HepG2 cells following knockdown of BCS1L and RISP, respectively.
5) Investigate effects of BCS1L downregulation on mRNA levels of chosen proteins involved in respiratory chain and iron metabolism.

2. Introduction

2.1. The Mitochondrion

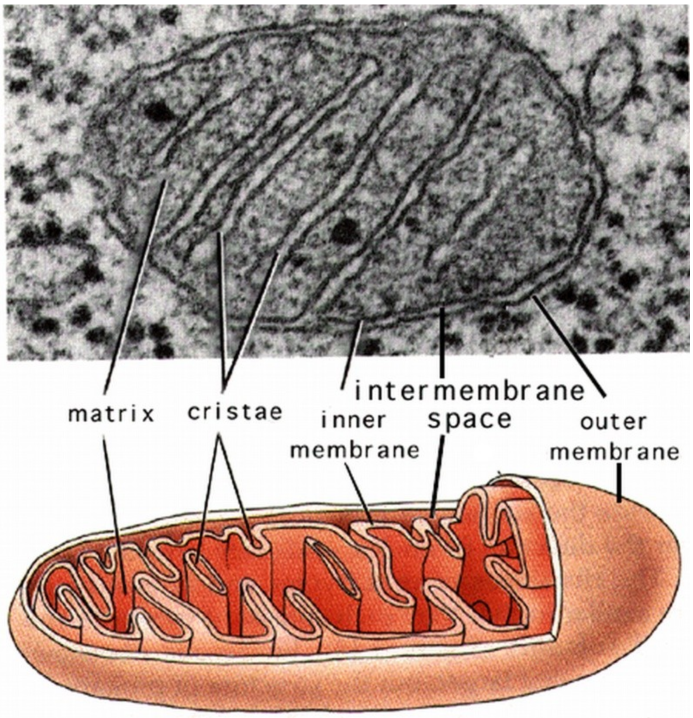

Fig. 1: Mitochondrial structure
(electron microscopy and scheme) (1)

Mitochondria are double-membrane organelles present in the cytoplasm of most eukaryotic cells. (2)
Morphologically, mitochondria consist of four compartments (Fig. 1); the outer membrane, the intermembrane space, the inner membrane and the matrix, the latter being the region within the inner membrane. The inner membrane is highly folded into cristae maximising the surface area. (3) Within the inner membrane the multiprotein complexes of the respiratory chain are located. The respiratory chain accomplishes the main function of mitochondria: the conversion of energy by oxidizing substrates and synthesizing the high energy adenosine triphosphate (ATP) molecule. ATP is the universal energy storage unit of the cells. (4)
In each human cell, except mature erythrocytes, there are hundreds to thousands of mitochondria depending on energy needs. (5) Therefore, tissues with a high energy turnover, such as brain, heart and skeletal muscle carry a big number of mitochondria. (6)
Mitochondria are fairly large, their size varies from smaller than 1µm to bigger than 4µm. (7) Furthermore, they are dynamic organelles which are constantly fusing and dividing. (8)

Mitochondrial DNA

The mitochondrion has its own mitochondrial DNA (referred to as mtDNA). It is the only organelle of the cell containing DNA besides the nucleus with nuclear DNA (nDNA). Each cell contains about five mitochondrial genomes with thousands of mtDNA molecules. (5)
Human mtDNA is a double-stranded, circular molecule with 16,569 base pairs (bp) coding for 37 genes. 13 genes of the mtDNA encode subunits of the respiratory chain and 24 of the them are used for mtDNA translation, 12S and 16S ribosomal RNAs (rRNAs) and 22 transfer RNAs (tRNAs). (9) MtDNA lacks introns, over 90% of the whole molecule are coding regions. (10)
Hence, the majority of the estimated 1000 to 1500 gene products within the mitochondrion (11), like most of the mitochondrial respiratory chain proteins and the mtDNA replication and expression systems are encoded by nDNA. (6) The proteins are synthesized in the cytoplasm and afterwards transported into the organelle. (11)
Mitochondria are passed on primarily by maternal inheritance, however, not as an absolute rule. (5)

Origin of mitochondria

The origin of mitochondria is still a controversial debate. Based on phylogenetic studies it is widely acknowledged that the mitochondrial ancestor evolved from the α-proteobacteria subdivision; probably a member of the Rickettsiaceaea family. (12)
The serial endosymbiosis hypothesis states that these bacteria were phagocytized by a host organism, either being a nucleus-containing eukaryote or an arachea. (13) Due to the rise of oxygen (O_2) levels in the atmosphere about two billion years ago, the anaerobic host needed an aerobic partner to survive under this condition. In addition throughout modification the significantly higher ATP yield by aerobic respiration was a major benefit to the cell. (12)
In contrast to the endosymbiontic hypothesis, the hydrogen hypothesis presumes that the first basic eukaryotic cell was a product of a hydrogen-producing

bacterium (the symbiont) and an anaerobic, hydrogen-depending methanogenic arachea (the host). Hydrogen was made accountable for the dependence of the host to the symbiont. Not endocytosis but gradually surrounding of the symbiont ended in the incorporation of the new organelle. (14)
In any case there has been a transfer from the mitochondrion ancestor's genome into the nuclear genome. Additionally, the genome of the intracellular symbiont gradually decreased within time of symbiosis and nuclear genes from the host were recruited for mitochondrial functions. (12)

Mitochondrial function

As mentioned above (and described in detail later on) the most important task of mitochondria is the generation of energy via the respiratory chain. However, mitochondria are involved in other pathways of cell metabolism and fulfil other fundamental tasks. (16)

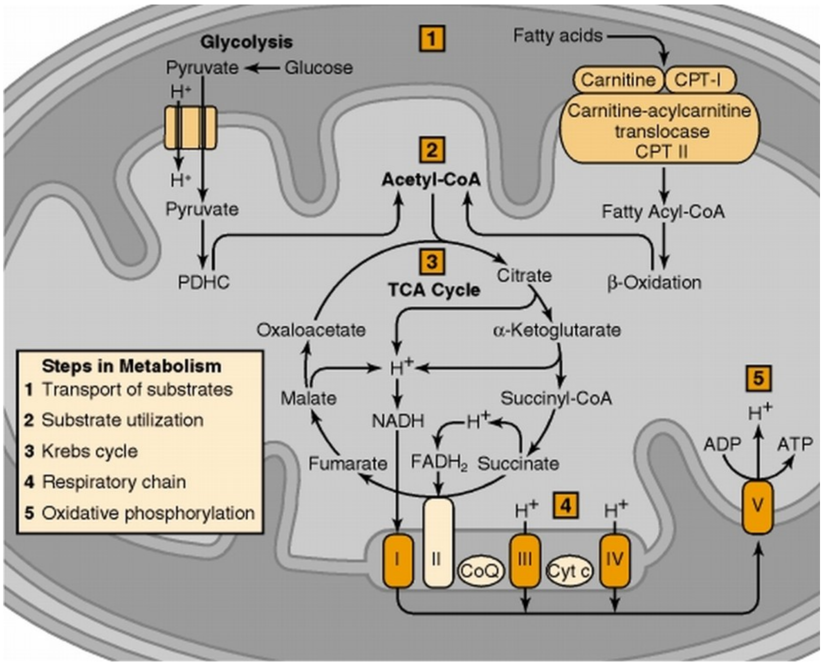

Fig. 2: Steps in mitochondrial metabolism (15)

The three energy sources of the human cell, carbohydrates (glucose), fatty and some amino acids are metabolised in catabolic processes to produce ATP. Most of these processes take place within the mitochondria. (Fig. 2) (17)
Under anaerobic conditions glucose is converted to lactate, which only has a small energy yield. (12) However under aerobic conditions glucose is converted to pyruvate via the glycolytic pathway in the cytosol. Afterwards pyruvate is transported into the mitochondrion through members of the mitochondrial carrier family. Pyruvate dehydrogenase located

within the inner mitochondrial membrane catalyzes the oxidization of puruvate to acetyl coenzyme A (acetyl-CoA). (18)

Fatty acids (FA) are degraded by β-oxidation. Fatty acids are carboxylic acids with at least eight carbon atoms. They are transported from the cytosol into the mitochondrial matrix via the carnitine palmitoyl transferase I (CPT-I) located on the inner side of the outer membrane and acylcarnitine translocase and carnitine palmitoyl transferase II (CPT-II) on the inner side of the inner membrane. Within the matrix β-oxidation takes place with four enzymatic reactions resulting in acetyl-CoA and a two carbon shorter FA. The cycle continues until the whole chain has been reduced to acetyl-CoA. (19)

Acetyl-CoA enters the tricarboxylic acid cycle (TCA) (also referred to as Krebs cycle and citric acid cycle). Through eight enzymatically catalized reactions the end products carbon dioxide (CO_2) and guanosine triphosphate (GTP) are generated. Additionally these reactions produce nicotinamide adenine dinucleotide (NADH) and flavin adenine dinucleotide ($FADH_2$) which are energy rich molecules containing a pair of electrons with high transfer and reducing potential. They enter the respiratory chain and are used to reduce molecular oxygen (O_2) to water (H_2O). (17)

Another major task of mitochondria is to produce reactive oxygen species (ROS). In fact they are the cells main source of ROS. They are generated in the respiratory chain, mainly within complex I and III. When O_2 is not fully reduced to H_2O superoxide anion ($O_2^{\bullet-}$), the general precursor of ROS occurs. Through dismutation hydrogen peroxide (H_2O_2) is produced. Interaction between the two molecules leads to the highly reactive hydroxyl radical (OH). About 1-2% of O_2 is converted into superoxide radicals during regular respiration. (20)

Excessive production of ROS results in mtDNA modifications, which are potentially mutagenic, might contribute to cancer, premature ageing and neurodegenerative disease. In addition ROS interact with mitochondrial proteins and lipids, damaging and impairing their function. (20)

Thus, it has an influence on the cells viability and evolves either in repair of the damage or in activation of apoptotic pathways. If the cell is going into programmed cell death ROS triggers the release of pro-apoptotic proteins, such as cytochrome *c* from the intramembrane space. (20)

On the other hand mitochondria possess multiple antioxidant enzymes to protect themselves from oxidative damage and furthermore apoptosis. The most important is the tripeptide glutathione, GSH (L-γ-glutamyl-L-cysteinylglycine) and multiple GSH-linked antioxidant enzymes. (20)

Furthermore, mitochondria are involved in iron metabolism; literally utilizing most of the cells iron. Iron is essential for cell life as a cofactor for many enzymes participating in metabolic processes. In the mitochondrion iron-sulfur clusters (FeS) and heme are synthesized as irons bioactive forms. (16)
Iron sulfur clusters are inorganic compounds resulting of the assembly of iron cations (Fe^{2+} or Fe^{3+}) and sulfide anions (S^{2-}) assisted by a series of cofactors. The clusters form either a rhombic [2Fe-2S] or cubic [4Fe-4S] cluster. Then they are incorporated into macromolecular structures involved in the respiratory chain, TCA cycle, regulation of gene expression and many others. (16)
Heme (iron-protoporphyrin IX complex) is a prosthetic group in many metalloproteins. They play a role in O_2 transport, the respiratory chain, signal transduction, metabolism and regulation. Heme itself can act as a regulatory molecule and affect transcription and translation. The biosynthesis takes place partly in the mitochondrion, partly in the cytosol. (16)
Next to its positive effects, iron can also be harmful; in the presence of O_2 iron is an effective inducer for the formation of ROS. (16)

Mitochondria are regulators in calcium (Ca^{2+}) homeostasis. Due to the negative potential of the inner membrane and a special uniporter Ca^{2+} is taken up zealously from the cytosol. When Ca^{2+} is transported out of the mitochondrion it is dependent on sodium (Na^{+}) in exchange. In general the fluxes in both ways are in balance. However, if the Ca^{2+} concentration in the cytosol rises over a certain critical set point, the fluxes are not balanced anymore and mitochondria start to uptake and accumulate Ca^{2+}, acting as very efficient cytosolic buffers. (21)
Mitochondria also play a role in steroid biosynthesis. The common precursor of steroids is cholesterol which is oxidized in various enzymatic steps requiring O_2 present in mitochondria. The early steps of steroid biosynthesis are controlled by cytosolic and mitochondrial Ca^{2+} levels. (21)

Last but not least mitochondria are responsible for the remodelling of mitochondrial proteins, the removal of damaged or unwanted proteins, the maintenance of mitochondrial DNA, (11) cell cycle control, development and antiviral response. (3)

2.1.1. Oxidative Phosphorylation (OXPHOS)

The mitochondrial respiratory chain is located within the inner mitochondrial membrane and is composed of five enzymatic multiheteromeric protein complexes, which are referred to as complex I, II, III, IV and V. (Fig 3) Each complex consists of a number of protein subunits which are mostly encoded, (approximately 77) by nDNA and only 13 subunits are encoded by mtDNA. (4) Since the majority of the proteins are encoded by nDNA they are synthesized in the cytosol and need to be translocated into the inner membrane. For this process they generally have a positively charged N-terminal amino acid sequences with amphiphilic features as a unique addressing signal which is later on removed by peptidases. (22)
The elaborate formation of the subunits to complexes with associated prosthetic groups and metal-containing reactive centres is conducted by a number of chaperones and assembly factors. (4) "Protein quality control" ensures the detection and removal of misfolded and wrongly incorporated protein formations which is essential due to such a great number of subunits. (22)
Secondary, there are two small electron carriers, ubiquinone (coenzyme Q10) and cytochrome *c*, a hemoprotein needed for proper respiratory chain function. These carriers are mobile and highly hydrophobic to be able to shuttle electrons between the complexes. Both are encoded by nDNA. (4)
The first four Complexes (C I-IV), the electron transport chain (mETC), are arranged in a specific orientation within the lipid bilayer of the inner mitochondrial membrane. They are responsible for electron transfer to O_2. The electrons are generated from reduced NADH and $FADH_2$ produced in the TCA cycle. Through a series of redox reactions releasing energy the electrons eventually interact with O_2, thus producing H_2O. (23)

Secondly, the complexes I, III and IV pump protons out of the mitochondrial matrix through the inner membrane into the intermembrane space. Due to the uneven distribution of protons a pH gradient and a transmembrane electrical potential of about 180mV with a negatively polarity at the matrix side is created (6), also referred to as proton motif force (pmf). The proton motif force activates and drives the synthesis of ATP conducted by complex V, the ATP synthase. (24) Hence, adenosine diphosphate (ADP) is phosphorylated through energy provided by protons flowing back to the matrix. (6)
The generation of ATP is coupled with carriers of adenine nucleotides (ANC) and inorganic phosphate (P_i) which provide the substrates for the ATP synthase. (22)

The five complexes

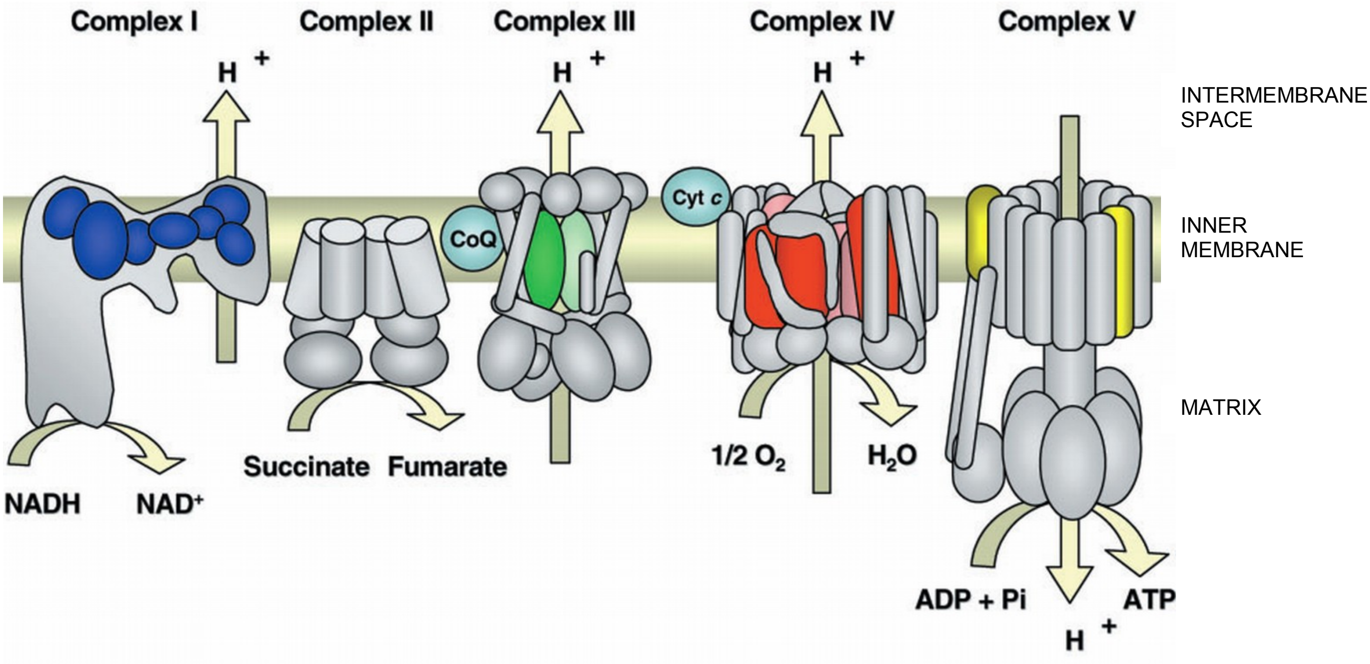

Fig. 3: Mitochondrial Respiratory Chain Complexes (4)

Complex I (NADH-ubiquinone oxidoreductase) is the by far largest of all complexes and consists of approximately 46 subunits, 7 encoded by mtDNA, about 39 encoded by nDNA. (4) Complex I accepts electrons from reduced NADH and oxidizes it to NAD^+ and H^+. Through a complicated series of redox reactions it eventually donates the electrons to ubiquinone, reducing it to ubiquinol. (25) The enzyme has an L-shaped structure containing two major domains (23), an extrinsic (hydrophilic) arm with one flavin mononucleotide, eight FeS centers and an intrinsic (hydrophobic) arm where ubiquinone is reduced. NADH is oxidated at the flavin mononucleotide and seven of the FeS clusters form a chain towards the ubiquinone binding site. Energy is conserved through one electron coming in and going out of complex I. The redox potential drops from NADH to ubiquinone, being able to translocate protons through the membrane. (26)

Complex II (succinate-ubiquinone oxidoreductase or succinate dehydrogenase) is built up by 4 subunits, entirely encoded by nDNA. (4) Complex II is at the same time a component of the TCA cycle. It oxidates succinate to fumarate and donates electrons to ubiquinone, as complex I does. (23)
Two membrane subunits (C, D) anchor two hydrophilic subunits (A, B), located on the matrix side, to the inner membrane. It has no cytosolic counterparts.
The subunit A of complex II has a covalently bound FAD prosthetic group and binds enzyme substrates – succinate and fumerate. The electrons obtained from succinate are transferred to several FeS clusters of subunit B. Then the electrons are transferred to a *b*-type cytochrome binding site in subunits C and D. Furthermore there are two binding sites for ubiquinone where electrons are delivered to the ubiquinone pool. (27) Complex II does not translocate any protons; it only participates in the respiratory chain by donating electrons. (23)

Complex III (ubiquinol cytochrome *c* reductase or cytochrome bc_1 complex) is made up of 11 subunits, whereas only cytochrome *b* is encoded by mtDNA. This complex transfers the electrons from ubiquinol to cytochrome *c*. (25) For each electron transferred to cytochrome *c* two protons are pumped across the inner membrane. (24)
(For more detailed description please see chapters Complex III and *BCS1L*.)

Complex IV (cytochrome *c* oxidase or COX) contains 13 subunits, COX I-III are encoded by mtDNA and the remaining 10 by nDNA. It catalyzes the reduction of O_2 to H_2O by reduced cytochrome *c*.
The subunits COX I-III are the catalytic subunits and compose the core of the complex. The active complex is a dimer with a number of prosthetic groups

involved for catalytic function: 2 hemes (α and $α_3$), two copper centers (Cu_A and Cu_B), zinc and magnesium.

The electron carrier, cytochrome *c* donates the electrons on the cytoplasmatic side of complex IV. Subsequently, these electrons are transferred to one of the copper centers (Cu_A), then heme α and finally to the active side, the binuclear heme-copper center ($α_3$-Cu_B), where O_2 is reduced to two H_2O molecules. (28) The necessary protons are provided by two channels on the matrix side. These channels are also responsible for the translocation of one proton per one electron across the membrane. (23)

Complex V (ATP synthase, F_0F_1 ATPase) consists of approximately 16 subunits, 2mtDNA, about 14nDNA encoded. (25) ATP synthase generates ATP coupled through the back-flow of protons to the matrix caused by the proton motif force. Nevertheless, the enzyme is able to work vice versa, hydrolyzing ATP and drive proton flow. (29)

The ATP synthase is combined of two small rotary motors, consisting of an electrical (F_0) and a chemical (F_1) motor. The F_0 portion is membrane embedded including the proton channel and the F_1 portion (referred to as “coupling factor”) (29) is H_2O soluble within the matrix with two parallel structures called “rotor” and “stator”. Protons flow through the channels across the membrane generating torque which moves the rotor and stator in opposite directions. (23) F_1 consists of three equivalent catalytic sites, when rotating one binds ADP and P_i, one processes them to ATP and one releases the synthesized ATP. (29) ATP synthesis is nearly to 100% effective, (23) generating three ATPs per twelve protons flowing back through the membrane. (30)

2.1.2. Mitochondrial Complex III

Complex III (ubiquinol cytochrome *c* reductase or cytochrome *bc₁* complex) is composed of two monomers with 11 subunits and 13 transmembrane helices to a symmetric dimmer structure. (31) The subunits are Core protein 1 and 2, six small subunits (all eight without redox prosthetic groups), and three polypeptides (subunits 3, 4, and 5) involved in electron transport: transmembrane subunit cytochrome *b* (cyt *b*) and two membrane-anchored subunits cytochrome c_1, (cyt c_1) and Rieske iron-sulfur protein (RISP). (32) These three polypeptides contain 4 metal redox centers in each monomer: heme b_H (with a high redox potential) and heme b_L (with a low redox potential) in cyt *b*, heme c_1 in cyt c_1 and a [2Fe-2S] cluster in RISP. (33), (23)

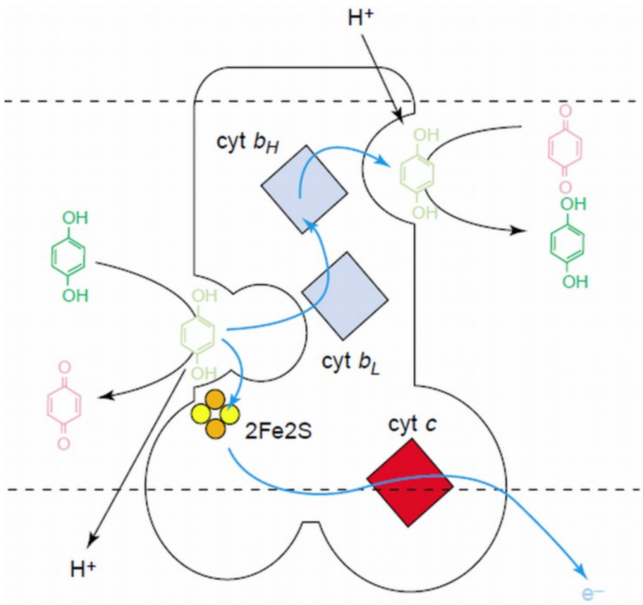

Fig. 4: schematic illustration of electron flow through the Q-cycle (24)

Complex III is responsible for the delivery of electrons from ubiquinol to cytochrome *c* (cyt *c*). The liberated energy through these reactions translocates protons across the membrane, which is referred to as Q-cycle (Fig. 4), first propsed by Peter Mitchell. (24) The complex has two quinone processing sites, called Q_o (quinol oxidase, also named Q_P for positively charged) on the outer surface of the membrane and Q_i (quinol reductase, also Q_N for negatively charged) on the inner side of the membrane and additionally three catalytic interfaces. (33), (23) Ubiquinol (QH_2) is oxidated at the Q_o site and the two released electrons bifurcate in two different paths. The first one goes along a high-potential chain to the RISP cluster, then heme c_1, which transfers it to the mobile carrier cytochrome *c*. When the RISP cluster delivers the first electron it undergoes a conformational change and moves away from the Q_o site closer to cytochrome *c*. On this account it is closer to cytochrome *c* and at the same time ensures that the second electron does not take the same path. (23) The removal of the first electron results in a semiquinone (SQ) at the Q_o site. Afterwards the second electron follows the low potential chain to heme b_L and b_H, which transfer it to the Q_i site. There the electron reduces either ubiqinone (Q) to SQ, or SQ to QH_2. (33) Hence, electrons going down the low potential chain are recycled and re-enter the Q-pool. (24) However, this process needs two electrons, therefore two ubiquinol molecules are oxidated at the Q_o site to eventually reduce one ubiquinone. (33) Q and QH_2 are liquid-soluble compounds able to diffuse across the membrane. The oxidation of QH_2 releases 4 protons and the reduction of Q needs 2 protons. (33) Consequently, the proton pumping stoichiometry is increased, 2 protons are translocated through the inner membrane for each electron transferred to cytochrome *c*. (24)

One side effect of the Q-cycle, however, is the formation of ROS. It might even be the cells major source. (33) Each time when QH_2 is oxidized by one electron a highly reactive intermediate SQ is generated. SQ reacts with O_2 to reduce it to superoxide anion ($O_2^{\bullet-}$). Under optimal conditions the Q-cycle is able to exceed this actual energetically favoured bypass reaction by some unknown mechanisms. Mutations in complex III or certain inhibitors can increase the creation of ROS considerably. (24) These inhibitors are antimycin A (Ama) binding to the Q_i site, inhibiting only one pathway and stigmatellin and myxothiazol both binding to the Q_o site. (33)

2.1.3. BCS1L

The *Bcs1* gene was first discovered in yeast Saccharomyces cervisiae. It encodes a mitochondrial protein which is anchored in the inner mitochondrial membrane. (34)
First it was found to be responsible for the expression of functional RISP. (34) Later on it was assigned the role as an ATP dependent chaperone for the proper assembly of complex III. (35)
For the generation of mitochondrial respiratory chain complexes a number of nuclear and mitochondrial encoded protein subunits and prosthetic groups need to be synthesised, inserted and assembled in a precisely coordinated way. To accomplish this there are a number of co-factors involved in the proper formation. Some of these co-factors are chaperones. (35)
Molecular chaperones are a heterogeneous group of proteins that assist in the non-covalent folding and unfolding, respectively assembly and disassembly of other macromolecular structures, without being a permanent component of this structure themselves. The absence of chaperones leads to incorrect interactions such as misfolding and misassembly resulting in biological non-functional products. (36)
Concerning complex III stable subcomplexes are generated in the first place to ensure stability against proteolytic attacks. Cytochrome *b* forms a subcomplex with Qcr7p and Qcr8p followed by Core1 and Core2. Cytochrome c_1 forms another one with Qcr6p and Qcr9p. These two subcomplexes combine to a cytochorme bc_1 precomplex.
Bcs1 protein (Bcs1p) gets involved in a late step of this process. It binds in an ATP-dependent manner to the precomplex and maintains it in a competent state for the assembly of RISP and subsequently, the small non-catalytic subunit Qcr10p. The incorporation is driven by ATP hydrolysis. The binding of Bcs1p to the precomplex prevents adverse folding and subunit interactions. However, Bcs1p does not play a role neither in the prior submitochondrial sorting of RISP, the incorporation of the FeS prosthetic group nor the assembly of Qcr10p. (35)
Bcs1p contains three different regions, the N-terminal domain, the Bcs1p specific domain and the C-terminal region. (37)

The N-terminal domain protrudes into the intermembrane space. The anchor to the mitochondrial membrane is only a single hydrophobic transmembrane domain. The majority of the protein is located as a tightly folded protease resistant domain in the matrix (N_{out}-C_{in} orientation). (38)
The N-terminal domain includes three distinct regions: the transmembrane segment, a presquence-like helix and an internal auxiliary region which are important for targeting of Bcs1p to mitochondria. The precursor Bcs1p is recognized by the TOM complex located in the outer mitochondrial membrane, it is imported into the mitochondrion and furthermore sorted and inserted into the inner membrane. (39)
The Bcs1p specific domain is significant for the activity and stability of the protein. (40)
The C-terminal region contains the AAA domain. (37) Bcs1p is a member of the AAA+ protein superfamily which are ATPases associated with different cellular activities. (35) These activities in the mitochondrion include: contribution to maturation and activation of proteins, general protein quality control, respiratory chain complex assembly and mtDNA maintenance and integrity. Thus, they have an important role in mitochondrial protein homeostasis. To perform these tasks the AAA+ proteins use energy of ATP hydrolysis. (11)
All these AAA+ proteins commonly have about 200 amino acids long domain encompassed by two sequences characteristic of ATPases and nucleotide binding proteins. (41)

In humans the analogue to the *Bcs1* gene in yeast is called *BCS 1-like (BCS1L*). *BCS1L* is located on the long arm of Chromosome 2 (2q33-37) (32) It is 1429 base pairs in length and its mass is 47.540 Daltons. (41) The *BCS1L* gene consists of seven exons and six introns. (42)
The BCS1L protein is built up of 419 amino acids (37) and between human and yeast there is a significant identity and similarity in protein sequence and conservation of functional domains. However, the N-terminals vary distinctively. (41)
BCS1L seems to be ubiquitously expressed in human tissues, with likely tissue-dependent differences in its expression. (42)

The well studied function of human BCS1L is the incorporation of RISP (22.000 Daltons) (43) and subsequently Qur10p into complex III of the respiratory chain. (35) However, other functions have been proposed. BCS1L could be accessorily responsible for complex IV maintenance since combined deficiencies of complex III and IV have been reported. (37) BCS1L probably plays a role in iron metabolism, maybe in biosynthesis and transport of iron clusters. (32) Additionally, there is some evidence that different mutations in *BCS1L* cause an increased production of ROS. (44) In human BCS1L knockdown cells mitochondria lost their network structures forming short, lumpy filaments with few branches. Thus, BCS1L seems to be responsible for the maintenance of mitochondrial morphology. Moreover, it caused downregulation of LETM1 (leucine zipper EF-hand-containing transmembrane protein 1), (45) a mitochondrial Ca^{2+}/H^{+} antiporter. (37)

BCS1L was investigated in mice during embryonic phase and showed an increased expression in critical regions for neuronal development. Therefore, it might also play part in the development of neuronal structures. (46)

The OMIM® - Online Mendelian Inheritance in Man® database, a compendium of human genes and genetic phenotypes assigned *BCS1L* the MIM (Mendelian Inheritance in Man) number *603647.

2.2. Mitochondrial Diseases

The first one to describe a mitochondrial dysfunction was Rolf Luft in 1962 at Karolinska Hospital, Stockholm, Sweden. His patient suffered of severe hypermetabolism of non-thyroid origin. The symptoms of the 35-year-old woman included: increased perspiration, polydipsia without polyuria, decreased body weight despite polyphagia, and progressing asthenia, which persisted since she was about 7 years old. (47)

Her basal metabolic rate (BMR) was over +100 per cent for many years and there were even peaks around +250 per cent. Additionally myopathy with muscular wasting and weakness, absent deep tendon reflexes, pathological electromyogram and creatinuria were found. In their biochemical studies Luft et al. focused on mitochondria and discovered increased amounts of mitochondria, a loosely coupled state of the oxidative phosphorylation and a major increase of total mitochondrial protein. Thus, he discovered the first mitochondrial disorder. (47)

Since then many mitochondrial diseases have been described in the literature. The estimated prevalence is 10 to 15 cases per 100.000 inhabitants. Mitochondrial diseases are therefore not as rare as commonly believed and the prevalence is about the same as well studied neurologic diseases such as amyotrophic lateral sclerosis or muscular dystrophies. (5)

Mitochondrial disorders are a very heterogeneous group. First of all, the diseases have multiple underlying pathogenetic mechanisms and secondly, different cellular and tissue expressions. (31)

Patients present with diverse clinical symptoms, ranging from lesions of single tissues or structures to more spread lesions including myopathies, encephalomyopathies, cardiomyopathies or complex multisystem syndromes. In general phenotypic expressions of mitochondriopathies are neurological manifestations such as neuromuscular and eye symptoms and movement disorders and systemic manifestations including heart, endocrine system, blood, mesenchymal organs and metabolism. (4)

The most common clinical presentations in paediatric patients are severe psychomotor delay, generalized hypotonia, lactic acidosis and sings of cardiorespiratory failure. (4) In pediatrics oxidative phosphorylation disorders are

usually inherited autosomal recessively, in general they result in server phenotypes and often fatal outcome. (25)
Diagnosis of mitochondrial disorders is challenging. In many cases it is necessary to perform muscle biopsies or fibroblast studies for bio- and histochemical analyzes. Additionally, genetic testing on muscle DNA might be essential since it is often not possible to detect the genetic defect in blood. (48)
Treatment options are limited to supportive measures. (48)

The mitochondrion is under dual genetic control, the nuclear and the mitochondrial genome. Disorders are inherited Mendelian and cytoplasmic way, respectively. (6)
In mtDNA mutations, deletions or rearrangements occur. (31) In general these changes are present in some, however not in all of the cells genome. Wild-type (normal) and mutant mtDNA are present (even in one single mitochondria), which is referred to as heteroplasmy. There is a certain threshold where a certain number of mutant mtDNA has to be present in order to cause dysfunction and clinical symptoms. (5) When cell division is carried out the mitochondria are redistributed randomly, consequently, the clinical symptoms may be tissue specific and vary with age. (31)
Most of the mitochondrial proteins are nuclear encoded. Mutations in structural components of the respiratory chain encoded by nDNA, however, are so far only observed in complex I and II and coenzyme Q10. There are approximately 60 ancillary proteins, which are important to the assembly or insertion of co-factors. Disease causing mutations of these co-factors have been reported for complex III and IV. It is assumed that mutations in structural subunits of complexes III, IV and V are lethal in utero due to lack of possible metabolic compensation. (5)

Mutations in the *BCS1L* gene have been discovered to be responsible for the majority of nuclear mutations leading to complex III enzyme deficiency resulting in three distinctive clinical phenotypes. First, GRACILE syndrome, lethal in the neonatal period, second Björnstad syndrome, associated with sensorineural hearing loss and pili torti and third complex III deficiency in neonates or infants, presenting with encephalopathy alone or with visceral involvement. (37)
Besides mutations in *BCS1L* additionally changes in only two subunits of complex III have been located to cause human disease. One gene, cytochrome *b*, is

encoded by mtDNA. There are frameshift, termination, deletion and missense mutations described. (49)

The second one is a nuclear gene, coding for the Qcr7p, subunit VII of complex III. It encodes the ubiquinone-binding protein. Instead of a mutation rearrangements of the gene occur, where amino acids are modified and added, respectively. (49)

2.2.1. The GRACILE syndrome

GRACILE syndrome (Fellman's syndrome, MIM #603358) is a lethal metabolic disease which has an autosomal recessive way of inheritance. The acronym signifies the main characteristics which are growth retardation, aminoaciduria, cholestasis, iron overload, lactic acidosis and early death. (50) It is caused by a point mutation in the *BCS1L* gene. (32) GRACILE syndrome is a member of the Finish Disease Heritage (FDH) (51)

In the 1960s the first known case with typical symptoms was born, in 1998 the clinical findings were described as a new distinctive neonatal disorder by Vineta Fellman. (50) So far 31 infants of Finish or Finish-born families have been diagnosed with GRACILE syndrome. The estimated incidence in Finland is 1:70,000 live births. (52)

Clinical Findings

Affected infants were born near term (mean 37.8 gestational weeks). (50) They were all small for gestational age; mean birth weight was 1670g, corresponding to an SD score of -4.0 for gestational age. (53) In contrast to infants with normal birth weight that is defined between 2500 and 4499g according to ICD10. The average birth length was 42.8cm and the head circumference 30.6cm. (50)

Intrauterine growth retardation is thought to develop in the second trimester. A discrepancy of about one week between the estimated delivery date calculated from the last menstrual period and the ultrasound biparietal diameter

measurements performed in the second trimester was noted. This resulted in correction of the estimated delivery date postponing it 1-2 weeks. (54)
At birth the first minute Apgar score was normal. Within the first days of life the patients developed fulminant lactic acidosis. At birth umbilical arterial pH was within normal range but decreased to an arterial pH of 7.0 or below (normal range 7.35-7.43). Base excess was around -22.5 (normal range -2; +2). Mean lactate was 12.3mmol/l (normal range: 0.7-1.8mmol/l), mean pyruvate was 121µmol/l (normal range 40-70µmol/l) and lactate pyruvate ratio was increased to an average 103 (normal value <25). (50)

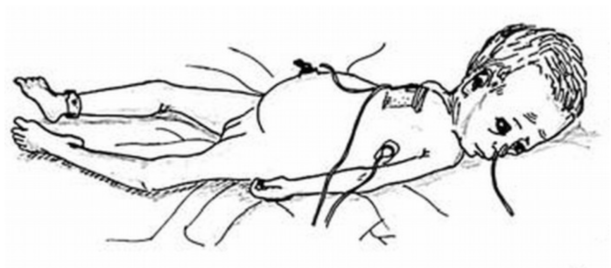

Fig. 5: GRACILE patient (55)

During the first day of life ultrasound of the liver showed normal size and structure. However, the infants developed intrahepatic cholestasis with progressive liver dysfunction shown by low thrombo-test values around 17 (normal >35), increased conjugated bilirubin concentration of 76µmol/l (normal <50µmol/l), increased alanine aminotransferase of 79U/l (normal <50U/l) and aspartate aminotransferase 151U/l (normal <50U/l). (50)
There was a server iron overload with consequently hemosiderosis of the liver. The abnormalities in iron metabolism included tenfold increased serum ferritin to 1890µg/l (normal range 10-250µg/l), decreased transferrin concentration to 0.72g/l (normal range 1.75-3.13) but full transferrin saturation of 86% (normal range 17-52%) and increased concentrations of soluble transferrin receptors to 20mg/l (compared to normal adult range 3-8 mg/l). (50)
Ultrasound of the kidneys did not reveal any structural abnormalities and there was no renal failure. However, in the urine nonspecific Fanconi-type aminoaciduria due to tubulopathy was detected. (50) The patients had losses of lactate, hydroxyphenyl-lactate, pyruvate, phosphate, glucose, (50) bicarbonate and carnitine in the urine. (53) It was not possible to detect free-carnitine concentration in the serum (normal range: 40-80µmol/l). (50)
No dysmorphic features have been observed. The infants looked very similar because of missing subcutaneous fat and wrinkled skin of the face. They have a “worried” facial expression. (Fig. 5) (50)

Neurological development showed no abnormalities. Muscle tonus was normal and no seizures appeared. (50) Ophtalmological examination revealed only twice mild cataract, otherwise it was normal if investigated. (53) Electroencephalogram, brain ultrasound and bran magnetic resonance were unremarkable. Cardiovascular function and echocardiographie were normal. There were no pulmonary or gastrointestinal problems. (50) Haemoglobin value and mean corpuscular volume of erythrocytes showed no abnormalities and no sideroblasts have been detected. (53)

All infants failed to thrive. No patient survived longer than 4 months. About the half of them died within the first three days of life and the other half between 2 weeks to 4 months. (53) Patients who died within the neonatal period had a rapidly progressive metabolic acidosis despite alkali treatment. The one who survived longer had less profound acidosis with short periods of normal arterial pH. There was hardly any weight gain and the infants died in an acidotic and cachectic state. (50)

The gender distribution in 25 patients was 17 girls and 8 boys. The boys survived a shorter time period which may indicates a more server disease in boys. (53)

Histopathological findings

The most impressive histopathological findings were in the liver. Intracellular and canalicular microscopic cholestasis was found in all investigated patients except one. In neonates there was paucity of intralobular bile ducts which could be the cause for cholestasis. All livers of infants who survived longer than one month presented macroscopically green color and increased firmness. They also showed increased fat accumulation in the liver. Firbrosis and steatosis developed parallel. There were an increased number of Kupffer cells containing large amounts of stainable iron granules, equally detected in hepatocytes. The iron granules decreased with the age of the patients. (56)

The pancreas appeared with intestinal fibrosis accompanied by exocrine atrophy. The majority of the patients had nephorcalcinosis which is relatively common in children below one year of age. In some cases tubular dysgenesis and the amount of proximal tubules were decreased to one tenth. (56)

Siderosis of macrophages in the spleen, lymph nodes, thymus, lung and pancreas was observed. All parenchymal cells except liver were negative for stainable iron, though. (56)
In autopsy studies the corpses showed severe wasting of somatic (muscular) organs. Massive pulmonary haemorrhage and hyaline membranes were present in some cases. (56)

Mitochondrial investigations

The lactic acidosis presenting in patients with GRACILE syndrome indicates mitochondrial dysfunction within the respiratory chain. (50) Given that *BCS1L* is the responsible gene for the GRACILE syndrome (32) its dysfunction causes the missing incorporation of RISP into complex III. (34) This defect in the assembly of complex III can be observed with Blue Native PAGE (BNP). (52)
Surprisingly, no obvious deficiency in complex III activity has been found.(50) Mitochondria have been isolated for investigation from muscle and liver specimen, from liver, brain, muscle, heart, kidney of urgent autopsies and moreover from patient fibroblasts. Complex III activity was measured indirectly in combination with complex I and II. (53) Furthermore active measurement of liver and muscle homogenates for complex III activity separately was carried out. Generally the activities were within normal range. (32)
Mitochondria in liver and muscle specimen investigated by electron microscopy appeared normal as well. (56)

Disease Locus

The GRACILE disease locus was detected to a restricted region 1-1,5cM between markers D2S2179 and D2S2244 of chromosome 2q33-37 using ancestral haplotype analysis and linkage disequilibrium. (57) Ancestral haplotypes are combinations of alleles of linked loci that are transmitted together on the same chromosome. When there is a non-random association of certain haplotypes the loci are in linkage disequilibrium. They occur more or less frequently in a population than would be expected. If the loci are tightly linked the decay can be quite slow. (58)

First *ABCB6* gene was excluded to be the cause for GRACILE syndrome. Due to functional and positional reasons it was suspected to be responsible. The *ABCB6* gene is involved in iron homeostasis, mitochondrial respiratory chain function and maintenance of mtDNA stability. However, no disease associated mutation was found and additionally, based on its location it could be excluded. (59)
In 2002 *BCS1L* gene (Fig. 6) was identified as the correct gene causing the GRACILE syndrome. In exon 2 of *BCS1L* a point mutation is located at position 232. Adenine is replaced by guanine (232 A>G) provoking a missense mutation. On protein level this exchange results also in an amino acid change where a serine is replaced by a glycine on position 78 (S78G). The disease appears when both alleles carry the mutation, i.e. the patient is homozygous for it. (32)

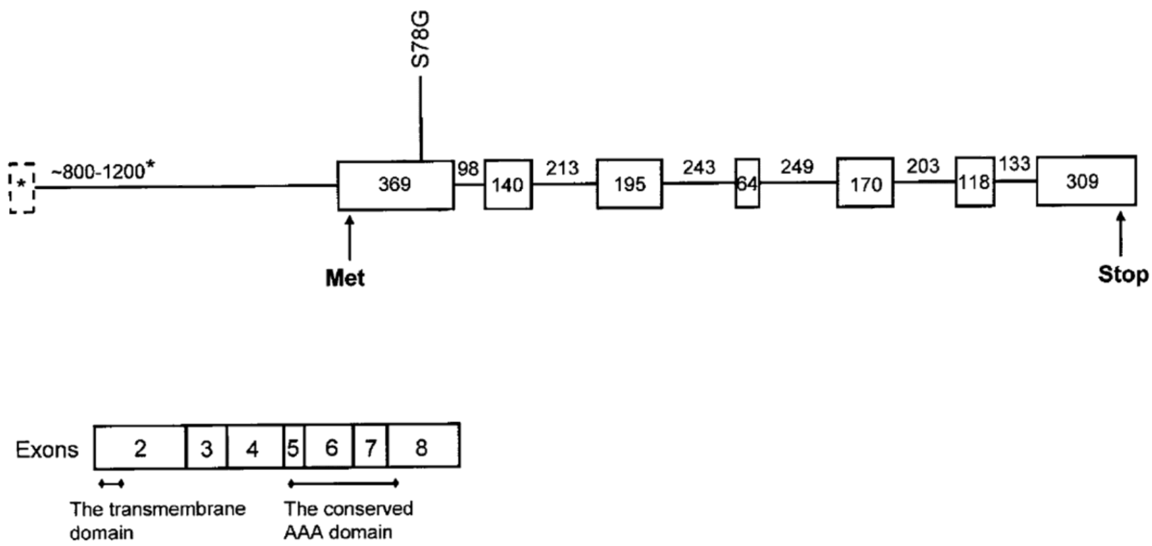

Fig. 6: Genomic structure of the *BCS1L* gene including the GRACILE mutation (S78G) with size of exons and introns indicated in bp. The BCS1L polypeptide with 419 amino acid residues. Modified from (32)

Treatment attempts

Due to its toxic effects free iron is suspected to be partly responsible for organ dysfunction. Therefore, a treatment protocol was developed with the aim to decrease free iron and iron overload in GRACILE patients. Apotransferrin infusions were administered to increase serum transferrin and followed by exchange transfusions. The two treated infants survived for several weeks, however, with no general improvement. So far there is no appropriate treatment for this fatal disease. (60)

Finish Disease Heritage

The GRACILE syndrome belongs to the Finish Disease Heritage (FDH), which is a group of at least 36 rare monogenetic diseases that are overrepresented in Finland. (51)

Today's about 5 million Finns (51) originated from only a small number of ancestors. The first settlers were Uralic speakers and migrated about 4000 years ago to Finland. However, the majority of the genes of the Finish population originated from a small Indo-European speaking founder population from the south arriving in Finland estimated 2000 years ago. This founder inhabited south-western costal regions of Finland which is referred to as the early settlement period. The population remained isolated mostly due to geographic reasons. In the 16^{th} century, about 50 generations ago an internal migration to middle, western, eastern and northern parts from a small south-eastern area occurred. This is termed late settlement. The migration formed rural populations which remained isolated for a long time. After repeated bottlenecks (famines and epidemics) the population expanded rapidly in the last three centuries. Based on these facts founder effect and genetic drift formed the gene pool of the population today. (61)

Overall genetic studies of the Finns showed a decrease in genetic diversity when compared to other European populations. (62)

Founder effect appears when a new population is established by a small group of people. In a small group it is likely that their genes are not representative of the general population. Thus the descendants may be different from the original population. (58)

The term genetic drift is used for cumulative changes in gene frequency due to sampling variation in small populations. When gametes are selected from a gene pool the sampling process happens at random. If the population is small “sampling errors” change the allele frequencies across the generations since the next generation is sampled from the current generation. (58)

If the descendant population remains small and isolated founder effect and genetic drift will result in fixation of certain allele frequencies, whereas some others are completely lost. (58)

Thus, the frequency of some rare diseases increased. On the contrary there are other genetic diseases such as phenylketonuria and cystic fibrosis which incidences are significantly lower or almost non-existing in Finland compared to the rest of Europe. (61)

In the subpopulations consanguineous marriages occurred, however, unknown to the individuals. In general several generations lay in between. This random inbreeding increased the incidence of rare recessive diseases. (61) Each one of the 36 diseases has its own distinct distribution, usually with a specific regional clustering and the majority have one suspected common founding ancestor. The mode of inheritance is typically autosomal recessive with only 2 being autosomal dominant and 2 being X-chromosomal. Most of these disorders present already in childhood with a wide clinical spectrum. Many diseases of FDH are a server handicap and burden to the patient and the family. About half of them are lethal at some point in time. (55)

Although overrepresented in Finland, in general FDH diseases are still rare. About 60 babies, 1 in 1000 live births, are born every year who suffer from a Finish disease. (51)

If an FDH disorder is found outside Finland (excluding places near the Finish border) the mutations differ from the Finish ones. (51)

The GRACILE syndrome is a member of the FDH. So far only patients from Finnish families and from one Swedish family with Finnish ancestry have been diagnosed. The map of Finland (Fig. 7) shows the birth places of the GRACILE patient’s ancestors and thus displays the distribution of the syndrome indicating the roots of these families are mainly within the area of the late settlement. (55) Although there is no tight clustering, most of the paternal and maternal ancestors of the patients could be traced to the same rural communities in eastern and central parts outside the densely populated areas of Finland. (50) It is assumed that there has been one single founding mutation for the GRACILE syndrome which has been introduced before the late settlement period more than 50 generations ago. (53)

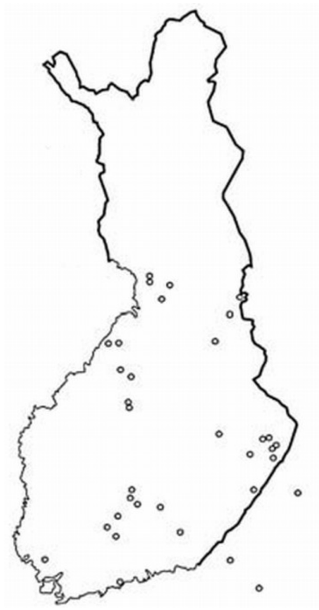

Fig. 7: Distribution of GRACILE patients in Finnland (55)

Possible effects of the GRACILE mutation

The GRACILE syndrome on the one hand is linked to BCS1L's function within the respiratory chain but on the other hand the phenotypic expression suggests functions of the protein in iron metabolism. Therefore, we investigated genes involved in hypoxia connected to ROS and the respiratory chain (HIF1α) and furthermore genes with essential functions in iron metabolism (Hepcidin, Ferroportin, Ferritin and TfrR2).

HIF-1 (hypoxia inducible factor 1) is a transcription factor and the main regulator of local cellular and systemic responses to hypoxia. (63) It is activated when O_2 levels decrease. As a consequence it triggers metabolic adaption and induction of new vascularisation through activation of the transcription of hypoxia-responsive genes. (64)
HIF-1 consists of the two subunits HIF-1α and HIF-1β. Both are continuously transcribed and translated. HIF-1β is constitutively stable expressed in contrast to HIF-1α which is under normal O_2 conditions degraded by prolyl hydroxylate enzymes (PHD). (64) The PHDs need O_2 as a substrate and iron as a co-factor. Mitochondria are sensors for hypoxia and respond with increased generation of ROS which then regulates a number of hypoxic responses, including the activation of HIF-1. In experiments cells with decreased RSIP levels failed to stabilize HIF-1α under hypoxic conditions. Thus, for this stabilization a functional mitochondrial transport chain and moreover H_2O_2 is required. (63) Overall it is assumed that the Q_o site of mitochondrial complex III acts as a regulator of HIF activation through a ROS dependent mechanism. Constitutively active HIF due to deficiencies in the degrading system lead to renal cell carcinoma. (64)

Hepcidin is a peptide hormone mainly synthesized in hepatozytes and the central regulator of the bodies iron metabolism. It is involved in the systemic absorption and remobilization of intracellular iron stores. (65) Hepcidin expression is induced by iron loading and inflammation (66) and downregulated by anaemia, hypoxia, erythropoiesis and furthermore, the hormone erythropoietin. Hepcidin itself induces the internalization and degradation of ferroportin. Deficiencies in hepcidin lead to several iron-related disorders. (65)

Ferroportin is a multipass membrane protein and responsible for cellular iron export, especially in the proximal duodenum, liver, spleen, (66), macrophages and cells of the placenta. It is the only known cellular iron exporter. (67) Ferroportin is a control for intestinal absorption. If missing erytrocytes accumulate iron inside them without being able to export iron to plasma. When hepcidin binds to the channel and causes its internalization, iron efflux into plasma is decreased. Ferroportin is essential for iron recycling. Mutations in ferroportin which lead to mislocation and degradation of the hormone cause iron accumulation in macrophages. (66)

Ferritin is the cytosolic iron-storage molecule of macrophages and other cells. (66) The ferritin core is able to contain up to 4.500 iron atoms. Fe^{2+} is the substrate for ferritin which oxidizes it to Fe^{3+} within its shell and stores it in this form. Ferroportin can deplete the cells of ferritin iron and subsequently leads to degradation of ferritin. (67)

Transferrin receptor 2 (TfR2) is a type II transmebrane protein. It binds to transferrin, the plasma iron transporter in a ph-dependant manner and mediates the cellular uptake of transferrin-bound iron. TfR2 expression is increased in liver hepatocytes. It is thought to play a role in iron homeostasis, since mutations in the TfR2 gene lead to iron overload diseases. (68)

2.2.2. Björnstad syndrome

The Björnstad syndrome (MIM #262000) was first described by Björnstad RT in 1965 as a new genetic entity. The disorder is associated with sensorineural hearing loss and pili torti. (69) It is caused by different mutations at various locations on the *BCS1L* gene. The mode of inheritance is autosomal recessive. (44) In contrast to the lethal disorders, the GRACILE syndrome and complex III deficiency the Björnstad syndrome is compatible with normal adult life. (70)
Pili torti are also referred to as “twisted hair” or “corckscrew hair”. It is a rare hair abnormality where the hair shafts are flattened at irregular intervals and rotated approximately 180 degrees around their axes. The hair appears to be sparse, coarse, dry, and extremely fragile. It breaks spontaneously; typically affected patients never need a haircut. However, eyebrows, eyelashes, axillary, pubic and body hair is usually normal. Generally Pili torti are recognized during the first 2 years of life. (71)
Sensorineural hearing loss varies from deafness to reduced hearing in defined frequencies (either low or high). It is nonprogressive prelingual hearing impairment. Patients are born with insufficient hearing and do not acquire speech normally. Some only communicate by sign language; others are able to use hearing aids and manage to have relatively normal speech. (69)
Major differences regarding age of onset and clinical severity have been observed. In general the most severe hair abnormalities also have the greatest hearing loss and vice versa. (71)
Associated signs of Björnstad syndrome might include mental retardation or hypogonadism. (70)

2.2.3. Complex III deficiency

18 infants from Britain, Turkey, Spain, Italy, Morocco and Finland and one woman from Kenya have been reported with different mutations in the *BCS1L* gene resulting in variable phenotypes. (72) (37) (73) This heterogeneous group is termed complex III deficiency. (MIM #124000) (74)
In general clinical manifestations include: low birth weight, metabolic acidosis at birth, proximal tubulopathy, hepatic involvement consistent with hepatic cytolysis or liver failure, muscular involvement and progressive neurological symptoms characterized by hypotonia, developmental delay and postnatal microcephaly. (72) (42) (74)
Most cases result in early death, especially when onset of symptoms at birth and servere enzyme deficiencies is reported. In contrast there are milder clinical courses with later onset of symptoms and longer survival, (37) up to date there is even one case of survival until adulthood. (73)
In accordance to this complex III activity ranges from no or mild defects in fibroblasts to severe deficiency in liver and muscle. (72)

The first three patients were three British infants presenting with decreased complex III activities; in addition two of the infants had decreased complex IV activity. Their symptoms included servere growth retardation, lactic acidosis, aminoaciduria, cholestasis in two cases and neurological problems including hypotonia and in one patient seizures. (32)
The first patient, a male died two days after birth. He was found to be a compound heterozygote for R565STOP (166C>T) - a premature stop codon at amino acid position 56 in exon 2 and V327A (1986T>C) - a missense mutation in exon 7. (32)
The second patient, a girl survived for 42 days. She had a heterozygous splice-donor mutation changing the first G of the second intron to a T (321G>T) and a T>A (-588T>A) heterozygous single-nucleotide change in the middle of the first intron, 588bp upstream from the start codon of *BCS1L* was detected. (32)
The last female patient carried two missense mutations as a compound heterozygote with S78G (232A>G) in exon 2 (the GRACILE mutation) and R144Q (529G>A) – a substitution of arginine to glutamine at codon 144 in exon 3. (32)

She presented with a milder disease than the GRACILE syndrome and died after 105 days. (31)

Another set of patients were six Turkish infants from four unrelated families were described. (42) They presented with lactic acidosis, neonatal proximal tubulopathy, hepatic involvement, normal or slightly decreased birth weight and significant encephalopathy, compartible with Leigh syndrome in one case. (31) Exept the last patient all other infants were born to consanguineous parents. (42)
Two affected siblings and one aborted fetus had a homozygous S227N (830G>A) change where a conserved serine was replaced by an aspartic acid in exon 5. The first born girl died at 3 months of age and the younger one was 9 years old at the time of publication with severe psychomotor retardation. (42)
Two infants from unrelated families but contagious parents had a homozygous mutation P99L (296C>T) - substitution of a leucine for a highly conserved proline. The boy died at 6 months and the girl at 2 years. (42)
The last patient was a compound heterozygote with R155P (464C>G) where an arginine was exchanged for a proline in exon 3 and V353M (1057G>A) a conserved valine replaced by a methionine in exon 7. The boy was still alive at 5 months, however, lost in follow up. (42)
The six patients had variable deficiency in complex III, which was measured in different tissues. Each mutation affected the function of the protein, however to different degrees, when it was introduced in yeast. (42)

A few cases have been reported in Spain. Clinically all of them had congenital lactic acidosis, failure to thrive, hypotonia and hepatopathy.
First of all, there were two Spanish siblings, a girl who died at 3 months and a boy who died at 3 weeks of age. An exacerbation of the situation with an acidotic crisis resulted in the fatal outcome. Additional symptoms included hypoglycaemia, encephalopathy and Toni Fanconi Debré syndrome. Complex III deficiency could be measured in liver tissue sample. Both infants were compound heterozygotes for R45C (246C>T) – substitution of arginine to cysteine at codon 45 in exon 2 and R56X (279C>T) – generating a premature stop at codon 56. (75)
Secondly, a Spanish girl was found with additional food intake intolerance, vomiting, proximal renal tubulopathy, microcephaly, bilateral cataracts and

nystagmus. She died with 6 months due to worsening of metabolic and neurological symptoms. Through analysis transitions in exon 1 paternally R45C (246C>T) and maternally R56X (279C>T) were detected. (72)
The last one was a 4 year-old boy who survived so far. He presented with growth and psychomotor retardation, abnormal subcutaneous fat distribution, hypertrichosis and sensorineural deafness as patients with Björnstad syndrome, however no hair abnormalities were noted. He suffered from a homozygous mutation in the first *BCS1L* coding exon resulting in a threonine to alanine exchange T50A (148 A>G). (74)

One Italian girl died of complex III deficiency at age 4 years. At birth she was small for gestational age, furthermore showed clinical signs of progressive encephalopathy, muscle hypotonia, spasticity, high frequency seizures, psychomotoric delay, dysmorphic features and brittle hair. The underlying mutations caused a compound heterozygote, R73C (217C>T) with an arginine exchanged to a cysteine in exon 1, inherited from the mother and F368I (1102T>A) phenylalanine replaced by isoleucine in exon 7 inherited from the father. (43)

An Moroccan girl was 4 years old and still alive at that time. At 9 months she presented with psychomotor regression, muscle hypotonia and failure to thrive. She had spastic quadriparesis and severe mental impairment. A brain MR showed brain atrophy. She additionally developed sensoneurinal hearing loss and had brittle hair – the symptoms of Björnstad syndrome. She was a compound heterozygote with two missense mutations a paternal R183C (547C>T) in exon 3 and a maternal R187C (550C>T). Both lead to an argentine exchange to cysteine. (43)

Three more patients were reported. The first one was a girl, who was still alive at the age of 4 and presented with typical symptoms of Björnstad syndrome, growth retardation, developmental delay and hypotonia. She had two mutations in *BCS1L* G35R and R184C. (44)
The second, a boy died at 11 months of age. He had clinical manifestations including lactic acidosis, tubulopathy, hepatopathy, hypoglycaemia, hypotonia,

failure to thrive and anaemia. It was a compound heterozygote for R56X (166C>>T) and 1181A>G and 1164C>G. (37)
The third one was a female, still alive at 5 years of age. Her symptoms were lactic acidosis, hepatopathy, encephalopathy, failure to thrive, seizures and spasticity in the upper and lower limbs. She suffered from a R184C mutation in one allele and a homozygous 1892 A>G, which was most likely not pathogenetic.(37)
Information about the nationality of the last three patients was not included.

Recently there has been a report on a 20-year old Kenyan woman with a new homozygous *BCS1L* mutation causing complex III deficiency. Primarily she was diagnosed with floppy infant syndrome. During development her condition severed, suffering from increasing muscle weakness, focal motor seizures and optic atrophy. Though, it seems that not all complex III deficiencies are fatal in childhood. (73)

2.3. Models for studying the disease

The group of Professor Vineta Fellman in Lund focuses on studying the effects of the 232A→G (S78G) mutation in *BCS1L* in order to understand its' role in the respiratory chain, iron metabolism and other possible, so far unknown, functions.
Therefore, they picked three different kinds of attempts.
Firstly, (my main project) we tried to establish a HepG2 cell model using RNA interference to study the pathways on a cellular and mitochondrial level, respectively.
Secondly, a genetic mouse model has been created to investigate the whole organism and the effects on different tissues.
Thirdly, isolated fibroblasts from patients who suffered from GRACILE syndrome were cultured and analyzed.

2.3.1. RNA interference

Cellular mechanism

RNA interference (RNAi) is a physiological process within the cells used to control gene expression by post-transcriptional silencing. So-called small interfering RNAs (siRNAs) induce the cleavage and degradation of their complementary target messenger RNA (mRNA). (76) RNA silencing is an evolutionarily conserved sequence-specific mechanism which is present in most eukaryotic organisms, from fission yeast, plants to mammals. (77)
The assumed physiological functions of siRNA are: antiviral defence (although viruses develop counter-defence strategies themselves), silencing mRNAs which are overproduced or translationally aborted, guarding the genome by suppressing the mobilization of transposons, (78) gene regulation and heterochromatin formation. (77)
SiRNAs are produced from long, double-stranded RNA (dsRNA) molecules. These dsRNAs emerge within the cells from replication of RNA viruses, from transcription

of convergent cellular genes or mobile genetic elements and from self-annealing cellular transcripts. (79)

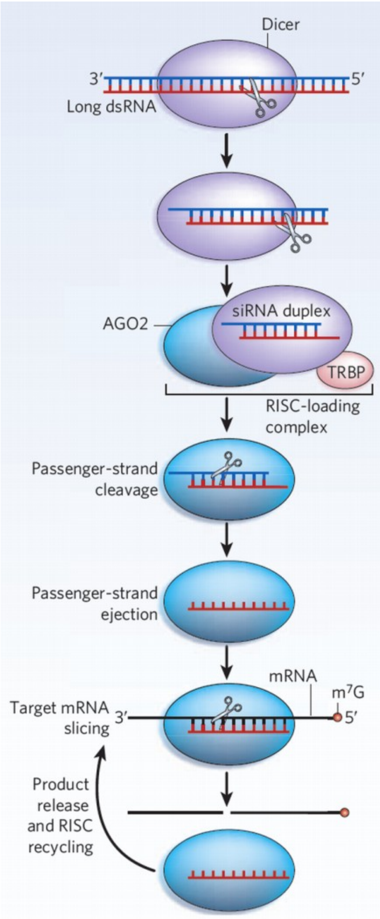

Fig. 8: human siRNA biogenesis and mechanism of action (79)

RNAi consists of an intracellular multistep process (Fig. 8) which is roughly separated into two phases, the initiation and the effector phase. (76)

In the initiation phase dsRNA molecules are cleaved in the cells by an endoribonuclease III-type protein named Dicer (DCR) into short 21-25 nucleotide double fragments. (80) These fragments are called siRNAs, short for small interfering RNAs however also referred to as small inhibitory (81) or short interfering (79) RNAs. On both 3'-ends the siRNA molecules have a two-nucleotide overhang and a hydroxyl-group and at each of the 5'-ends a phosphate group. (76)

The Dicer is a multidomain complex which is about 220 kDa (Fig. 9). It consists of a DExH RNA helicase/ATPase domain, a DUF283 and a PAZ domain, two neighboring RNAase III domains (RIIIa and RIIIb) and a dsRNA binding domain (dsRBD). (82) The two neighboring RNAase III domains form an intramolecular dimer acting as a monomer (80) to function as a single reaction centre which cleaves simultaneously both strands of the dsRNA. (82) Dicer probably uses a two-metal-ion mechanism to catalyse RNA cleavage. (79)

DsRBD is a domain which mediates unspecific interactions with dsRNA. (82) The DUF283 (Domain of Unknown Function 283) is thought to be responsible for siRNA strand selection, whether by direct identification of the asymmetry of RNA duplexes or recruiting another dsRBD domain. (83) The PAZ (Piwi/Argonaute/Zwille) (84) domain is an RNA-binding domain which specifically recognizes and binds the 3'-end 2nt overhangs of single stranded siRNAs. (79)

The distance between the PAZ domain and the RNAase III dimer is 21 (85) to 25 (80) base pairs long. Consequently, the Dicer operates as a molecular ruler. (Fig. 9) (80)

In the second phase, the effector phase, after Dicer mediated cleavage the siRNAs are incorporated into the RNA-induced silencing complex (RISC) which is a nuclease-

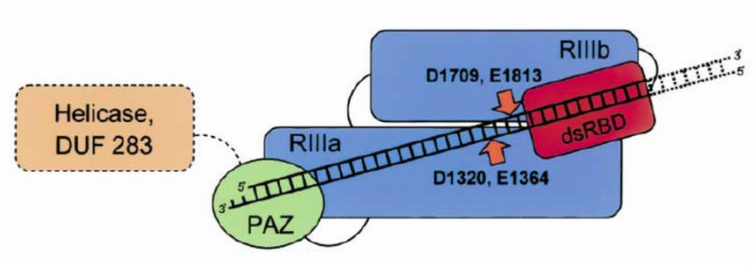

Fig. 9: model for dsRNA processing by Dicer (82)

containing multiprotein complex. (76) The assembly of RISC is initiated by the RISC loading complex (RLC) recruiting the siRNAs leading to the eventual transition into active RISC. (78) RLC consists of an Argonaute (AGO) protein, Dicer and a dsRBD-containing protein TRPB. (79) The siRNA douplex is loaded onto the AGO protein where it is unwound. One strand of the siRNA is selected as the guide strand based on the thermodynamic asymmetry rule. (80) Meanwhile the non-guide or passenger strand is cleaved by the AGO protein and an endonuclease C3PO ejects the cleavage products. (86) This slicing of the passenger strand provides the energy required for unwinding the RNA duplex and loading the guide strand onto RISC. (80)

The AGO protein family are the core components of the RISC complex. In humans there are four AGO proteins (AGO1, AGO2, AGO3, AGO4) (79) whereas only AGO2 has slicer activity and can cleave the target mRNA. (78)

The human AGO proteins have four domains: N-terminal domain, PAZ domain, middle Lac-Z like (MID) domain, PIWI domain. (85) The PAZ domain binds to the 3'end of the guide strand and the RNase H-like PIWI domain contains the silencing active site in AGO2. (86)

The AGO protein conducts the siRNA guide strand to the perfectly complementary target mRNA. Base pairing occurs within the 3'-untranslated region (UTR) of the mRNA. (86) The endonucleolytic cleavage of mRNA catalyzed by the AGO protein is a process known as silencing. (79) Phosphodiester bounds within the polynucleotide chain are cleaved. Due to this, RNA ends are not protected, which results in rapid degradation of the mRNA molecule. Thus, this prevents the expression of the corresponding gene and therefore protein translation. (76)

Besides cleaving RISC, there is another type which is non-cleaving RISC. It depends on the type of loaded AGO protein. Therefore, the assembly of RISC leads to either cleavage of the target mRNA and translational repression, respectively in case of non-cleaving RISC. (78)

Next to siRNAs there are also microRNAs (miRNAs) and PIWI-interacting RNAs (piRNAs) interacting in the regulation of gene expression. These three form the main classes of small regulatory RNAs. (79)
Micro RNAs (miRNAs) are about the same length as siRNAs and are encoded in the genome. They evolve from stem-loop structure transcripts, also cleaved by the Dicer. However, they are only partly complementary to their target mRNAs and therefore AGO proteins do not slice the mRNA. It is thought that deadenylation (removal of the poly(A)tails of mRNA) leads to mRNA degradation. (79) MiRNAs play a regulatory role in gene expression and furthermore are essential for growth and development of an organism. (78)
PiRNAs are responsible for silencing transposons in animal germ cells. (79)

RNAi has been discovered and first described in *Caenorhabditis elegans* in 1998. RNA was experimentally introduced into cells to interfere with the function of an endogenous gene. It was observed that dsRNA are very effective in interference in contrast to purified antisense and sense RNAs individually which only were able to produce marginal effects. (87)
Interestingly, RNA silencing process is able to spread from cell to cell and also on long distances to cause systemic RNA silencing in whole organisms. This is accomplished by a sequence-specific silencing signal after the introduction of RNA silencing in single cells. (77)

Experiments with siRNA

For experimental reasons synthetically produced siRNAs can be directly introduced into the cells where the initation phase is omitted. (76)

Guidelines to design siRNAs with best results in efficacy and specificity have been established through several studies. Synthetic siRNA length should be 25-30 nucleotides, which is longer than physiological siRNAs. However at this length they are substrates for Dicer and thus are directly incorporated into RISC. (76)

Additionally, a low G/C content (36% to 52%) and symmetric 2nt overlaps at the 3'-ends are important. There are several positions where specific nucleotides show better results – to mention one, nucleotide 10-11 represent the RISC mediated cleavage of the target mRNA, likewise other endonucleases it preferably cleaves a 3' U rather than the other nucleotides. (76)

Any internal repeats or palindrome sequences should not appear because they lead to intramolecular fold back structures which are then missing for the silencing process. (76)

Using siRNAs includes a risk of nonspecific ("off-target") effects which include mRNA degradation, inhibition of translation or induction of an interferon response. (81) The siRNAs may cross react with targets of limited sequence similarity when regions of partial sequence identity between the target mRNA and siRNA exist. (76)

Additionally the interferon system might be induced when dsRNA molecules enter the cells activating a multi-component signalling complex. In most cases this happens to long dsRNA, the siRNAs are usually too small; however, the effect seems to depends on their sequence. (76)

Therefore it is important to use the lowest possible siRNA concentration which still creates the desired effect and optimized siRNA delivery methods. (76)

When performing siRNA experiments several controls need to be included for correct interpretation of the results. (88)

First, it is essential to use a positive control which is known to provide a high knockdown of its target gene. One option is to use Cell Death control siRNA which knocks down ubiquitous human cell survival genes. This results in cell death of most of the cells possible to investigate by light microscopy. The positive control

ensures that transfection and knockdown analysis are working optimally when an experimental set up is established. (88)
Starting RNAi experiments in a new cell line transfection control should be used to determine efficiency. It can be measured either by fluorescent microscopy after transfection with a fluorescently labeled siRNA or by observation of cell death after using siRNA directed against cell survival genes. (88)
If the siRNA causes changes in phenotype it has to be confirmed by additional siRNA directed against a different area of the same mRNA. (88)
Besides these optimization controls, each experiment in general should include a negative control, mock transfection control and untransfected cell control. A negative control siRNA is a nonsilencing RNA designed with no homology to any known mammalian gene. This siRNA is incorporated into RISC and shows only minimal nonspecific effects on gene expression and phenotype. Thus it helps to determine any nonspecific effects caused by siRNA transfection. Furthermore, mock transfection control has to be carried out where siRNA addition is omitted. This control includes transfections with the transfection reagent only. Additionally, an overall untreated and untransfected cell contol should be used for gene expression analysis to determine the normal, basal expression rate. (88)

The HepG2 cell line

HepG2 cells are a human-derived liver carcinoma cell line. It was first established in 1979 cultured from liver biopsies from a primary hepatoblastoma of an 11-year old Argentine male. (89)

The morphology of the cells is small, dark, rather uniform and fetal-type epithelial. (90) They resemble human hepatocytes, synthesize and secrete many of the plasma proteins characteristic for them (89) and in general express a wide variety of liver specific metabolic functions. (90) The karyotype of HepG2 cells is aneuploidic with a range of 48-54 chromosomes per cell. (89)

Since the liver is the target organ of GRACILE syndrome this cell line has been chosen for experiments. Additionally, HepG2 cells are very rich in mitochondria and therefore, are a good model to study mitochondrial respiratory chain function and its diseases. (91)

An advantage of the cell line is that the cells grow adherent on the Petri dish. On account of this they are not affected by changing the culture media they are grown in, unlike cells that are grown in suspension which are largely removed when the medium is exchanged. Hence these cells can be cultured longer and the time the cells are exposed to the medium containing an agent can be defined for a long period. (91) The generation time of HepG2 cells is 20 to 28 hours. (89)

HepG2 cells are continuously growing, tumor cells and differ from normal, resting, non-neoplastic cells. However, they are quite easy to study and can provide good hints how physiological cells function. Furthermore, it is possible to investigate the pathways on cellular level when the cells are manipulated in one way or the other. (91)

3. Materials and Methods

3.1. HepG2 cell line

HepG2 cells were grown on 10cm Petri dishes in a cell incubator with 37°C temperature and 5% CO_2 concentration in 10ml growth medium GIBCO™ RPMI Medium 1640 + GlutaMAX™ from Invitrogen™. Beforehand 10% fetal bovine serum (FBS) and 1% Penicillin/Streptomycin (PS) were added to the medium. It was changed approximately on 3 day intervals and the cells were split regularly when reaching about 80% confluency. To maintain best conditions for experiments, cells were passaged two days prior to start of experiments.
In order to split the cells, medium was removed and the cells were washed with phosphate buffered saline (PBS). Then 1ml of Trypsin, a serine protease, was added to the cells and incubated for 5 minutes to detach the cells from the dish. The cells were harvested, centrifuged, counted via microscope and cell counter, resuspended in medium and reseeded on the Petri dishes.

3.2. RNA interference using siRNA

For our experiments we used two kinds of siRNAs, whereas the first ones were directly targeted against *BCS1L* mRNA and the second ones against *RISP* mRNA.
The conducted experiments against *BCS1lL* mRNA included Hs_BCS1L_2_HP siRNA whose target sequence is: CCG CAT TTC CAC TAA GTT TGA. The sense strand being: r(GCA UUU CCA CUA AGU UUG A)dTdT and antisense: r(UCA AAC UUA GUG GAA AUG C)dGdG. The second siRNA used was Hs_BCS1L_4_HP siRNA, target sequence: CCG AAT TGT CAG AGA CGT CCA, sencse strand: r(GAA UUG UCA GAG ACG UCC A)dTdT and antisense: r(UGG ACG UCU CUG ACA AUU C)dGdG.
The siRNA directed against *RISP* mRNA was Hs_UQCRFS1_6_HP siRNA with a target sequence of: TAG ATA GTA CGA AGT CTT CAA, sense strand:

r(GAU AGU ACG AAG UCU UCA A)dTdT and antisense r(UUG AAG ACU UCG UAC UAU C)dTdA. Moreover, we designed an siRNA directed against *RISP* mRNA ourselves, where we chose the target sequence: AAT GCC GTC ACC CAG TTC GTT, sense strand: r(UGC CGU CAC CCA GUU CGU U)dTdT and antisense: r(AAC GAA CUG GGU GAC GGC A)dTdT. The "dTdT" ends stand for DNA ends which are added to the siRNAs to improve the knockdown function.

SiRNAs were purchased from Qiagen®. The lyophilized (freeze-dried) siRNA was diluted with siRNA Suspension Buffer provided by Qiagen® to obtain a 20µM (250ng/µl) stock solution. This solution was heated to 90ºC for 1 minute and then incubated for 60 minutes at 37ºC. SiRNA solution was aliquoted and stored at -20ºC. (88)

Besides siRNA and medium (without added FBS and PS), a Transfection Reagent is part of the siRNA transfection process of mammalian cells which is used to deliver siRNAs into the cells. For our experiments we applied HiPerFect Transfection Reagent from Qiagen® (in the following referred to as "HiPerFect"). According to the Qiagen® protocol low siRNA concentrations can be used with HiPerFect to still achieve high efficient knock down. HiPerFect has a low cytotoxity and the cells remain healthy and viable during the experiments. (88)

For transfections of HepG2 cells the "Fast-Forward Transfection" Protocol was chosen. (88) Following this protocol, cells were seeded and transfected on the same day. SiRNA was diluted in 100µl serum-free medium; in general we used a concentration of 5nM. Afterwards HiPerFect was added and mixed by vortexing. To obtain formation of transfection complexes, the samples were incubated at room temperature for 5 to 10 minutes. Subsequently the complexes were added drop-wise onto the cells and distributed by swirling. Cells were incubated at 37°C temperature and 5% CO_2 concentration. Medium was changed every day if necessary for experiments lasting for several days.

In the beginning several optimization experiments were preformed to determine the best knockdown conditions. For these experiments cells were seeded on 12-well plates each well containing 1.100µl medium. We analyzed the number of cells (150.000 vs. 75.000), the concentration of siRNA (1nM, 5nM vs. 10nM), the amount of HiPerFect (3µl, 6µl vs. 9µl) and the number of days after transfection (1, 2, vs. 3 days).

After these optimizations steps we proceeded to transfecting cells in 6cm Petri dishes. We used 400.000 cells in 4.000µl medium, 20µl HiPerFect and 5nM siRNA. For those experiments we retransfected the cells up to three times on two day intervals.
HepG2 cells transfected with siRNA were always compared to HepG2 cells transfected with only HiPerFect (referred to as “untreated HepG2 cells”) to ensure the Transfection Reagent does not cause any unspecific effects itself.

3.3. *BCS1L* & *RISP* mRNA expression

3.3.1. RNA preparation

Following the experimental period HepG2 cells were harvested and Quaigen® RNAeasy® Mini Kit was used for purification of total RNA. (Fig 10)
10µl β-mercaptoethanol was added to 1 ml RLT lysis buffer, containing the harmful guanidine-thiocyanate, responsible for disruption of cell walls and plasma membranes of cells and organelles, denaturation, and furthermore inactivation of RNases to ensure the purification of intact RNA. (92)
Cells from which medium had been completely removed were lysed with approximately 350µl of RLT buffer including β-mercaptoethanol. The cell lysate was added to a QIAshredder homogenization spin column placed in a 2ml collection tube. Homogenization is needed for the reduction of viscosity of the lysate. It dissects high-molecular-weight genomic DNA and other cellular components to obtain a homogenous lysate. Otherwise RNA would not be able to bind effectively to the RNeasy membrane later on. (92)
The QIAshredder column was centrifuged with a microcentrifuge for 2 minutes at maximum speed. 70% ethanol was added to the lysate and mixed well by pipetting. Ethanol is essential for selective binding conditions for RNA to the RNeasy membrane. (92)

Afterwards the sample was applied to an RNeasy spin column placed in a 2ml collection tube. Total RNA bound to the membrane and all the contaminants were efficiently washed away in the following steps. The column was centrifuged for 15 seconds at 8.000xg (gravitational force) equal to 10.000 rpm (revolutions per minute). Then the flow through was discarded.

700µl RW1 buffer was added to the column and again centrifuged for 15 seconds at 8.000xg to wash the spin column membrane. The collection tube was removed and the RNeasy column transferred into a new 2ml collection tube. 500µl RPE buffer was then pipetted onto the column and it was centrifuged for 15 seconds at 8.000xg. The flow through was discarded. Then another 500µl RPE buffer was added as a last washing step and everything centrifuged for 2 minutes at 8.000xg. The RNeasy column was transferred to a new 1,5ml collection tube. RNA was eluted by adding 50µl RNAse free H_2O to the column and centrifuged for 1 minute at 8.000xg. RNA needed to be placed on ice as fast as possible to prevent degradation. (92)

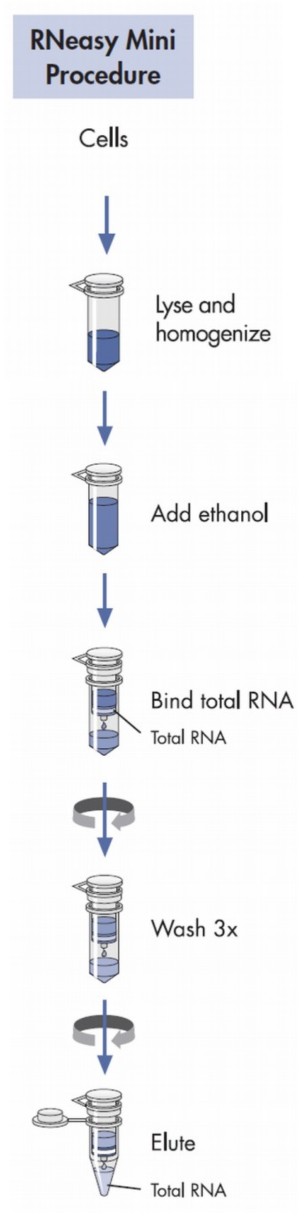

Fig. 10: RNA preparation
Modified from (92)

RNA amount was measured via NanoDrop™ ND 1000 spectrophotometer at 260nm. Therefore 1µl of undiluted RNA was placed on the lower measurement pedestal. After the upper optical pedestal was lowered, it engaged with the sample, forming a liquid column. Two defined path lengths, 1 and 0.2 mm between the two optical surfaces, were used for each measuring cycle. RNA is measured by using fiber optic technology and surface tension properties. (93) According to the measurement the RNA samples were diluted with H_2O to 50ng/µl. RNA molecules longer than 200 nucleotides are purified with this procedure. Therefore, especially mRNA is present in the samples, because most other RNAs like 5.8S and 5S rRNAs and tRNAs, which are 15 to 20% of total RNA, are shorter than 200 nucleotides. (92)

3.3.2. Two Step real time PCR

To quantify gene expression of *BCS1L*, *RISP*, and other genes of interest two-step real time polymerase chain reaction (PCR) was performed. (Fig. 11) In the first step complementary cDNA (cDNA) was reverse transcribed from total RNA samples. In the following PCR step, the cDNA template was used to create PCR products for quantification.

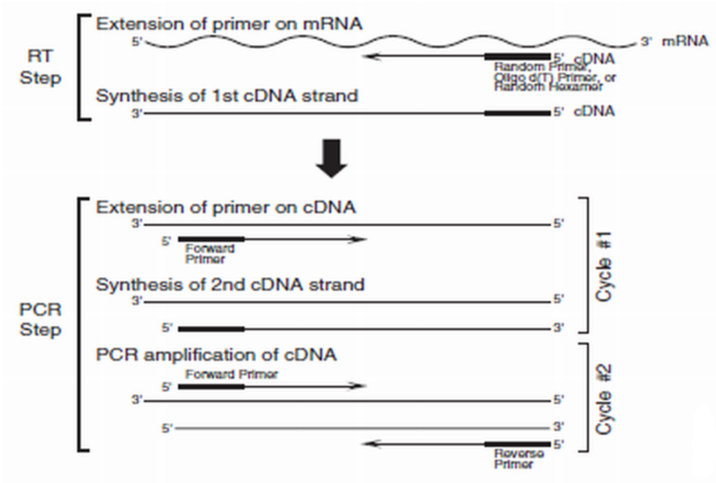

Fig. 11: Two-step RT PCR, first cDNA synthesis and subsequently amplification via RT-PCR (94)

cDNA Synthesis

A complementary DNA (cDNA) template was created via reverse transcription reaction. During this process mRNA was converted into single-stranded cDNA, due to the fact that DNA is much more stable than RNA for further analyses of the mRNA template via real time PCR. (95)

The TaqMan® Reverse Transcription Reagents were purchased from TaqMan® by Applied Biosytems™.

For cDNA snynthesis a mastermix of 5µl 10xTaqMan RT buffer, 11µl 25mM Magnesium Chloride, 10µl deoxyNTPs mixture, 2,5µl Random Hexamers, 1µl RNAse Inhibitor, 1,25µl MulitScribe™ Reverse Transcriptase (50U/µl) and 9,25µl RNAse free H_2O for each sample was made. (96)

Random hexamers, a mixture of random hexanucleotides with 5' and 3' hydroxyl ends being the primers (97) and MulitScribe™ Reverse Transcriptase being a recombinant RNA-dependant polymerase which uses single-strand RNA in combination with a primer as a template to synthesize a cDNA strand. (98)

Importantly, all the reagents needed to be kept on ice. Then 50µl of the mastermix was distributed in MicroAmp® Optical 8-Tube Strips, 0.2ml. To each of the tubes 10µl of 50ng/µl RNA template was added. Additionally, one undiluted RNA template was also enclosed to be used for a standard curve for real time PCR. The Tubes were closed with MicroAmp® Optical Caps. The strips were centrifuged briefly to avoid any air bubbles and ensure the liquid being at the bottom of the tube. (96)

The tubes were placed in the thermal cycler block. The PCR (polymerase chain reaction) machine was programmed first 10 minutes at 25°C for primer incubation, which is necessary for maximum primer-RNA template binding, when random hexamers are used. Then 30 minutes at 48°C for reverse transcription and cDNA synthesis and as the last step 5 minutes at 95°C for reverse transcriptase inactivation. (96)

cDNA amount was measured via NanoDrop™ and the samples were stored at -20°C.

real time PCR

In the second step the cDNA template was amplified with real time PCR using ABI Prism® 7000 Sequence Detection System. Real time PCR enables to monitor the PCR progress as it occurs and meanwhile collect data during the whole process. In order to detect PCR products there are fluorescent chemistries which correlate PCR product concentration to fluorescence intensity. (99)

To perform real time PCR cDNA templates were diluted 1:4. For each sample a mastermix of 12,5µl TaqMan® Universal PCR Master Mix 1,25µl TaqMan® Gene Expression Assay Mix (20X) and 7,25µl RNAse-free H_2O was prepared. TaqMan® Universal PCR Master Mix contained AmpliTaq Gold® DNA Polymerase, AmpErase® uracil N-glycosylase (UNG), dNTPs with dUTP (deoxyuridine triphosphate), passive reference and optimized buffer components. (96) TaqMan® Gene Expression Assay Mix (20X) contained forward PCR primer, reverse PCR primer and TaqMan® probe. (94) The applied assays were BCS1L Hs00188932_m1 with an amplification length of 95bp of a coding region, RISP Hs00705563_s1 with an amplification length of 85bp of a coding region, beta actin (ACTB) Hs99999903_m1 with an amplification length of 171bp also of a coding region and furthermore assays for genes involved in iron metabolism (HIF1α, Hepcidin, Ferroportin, Ferritin and TfrR2). All assays were purchased from Applied Biosystems™. (100)

The prefix indicated the species; “Hs” for Homo sapiens. The suffix indicated the assay placement. “m” was a probe which spaned an exon junction and “s” was a probe which primers were designed within a single exon and therefore detected by definition additionally genomic DNA. (100)

ACTB is a housekeeping gene, an endogenous control as an active reference to standardize the amount of mRNA target added to each reaction. It is supposed to have a relatively stable expression throughout treatments of cells. (101)

A standard curve of known concentrations of a stock cDNA with a dilution series of 1:1, 1:5, 1:25, 1:125, 1:625, (1:3125) and 1:15625 was made for each the target and the endogenous control sample.

The mastermix was pipetted into a MicroAmp® Optical 96-Well Reaction Plate and the templates were added and mixed. Each sample including target, endogenous control, no template control (NTC) that is H_2O and all standard curves were doubled. The MicroAmp® Optical 96-Well Reaction Plate was sealed and centrifuged to avoid air bubbles. For the PCR reactions ABI Prism® 7000 Sequence Detection System was set to 50°C for 2 minutes, then 95°C for 10 minutes following 40 cycles of 95°C for 15 seconds for denaturation and 60°C for 1 minute for annealing and extension.

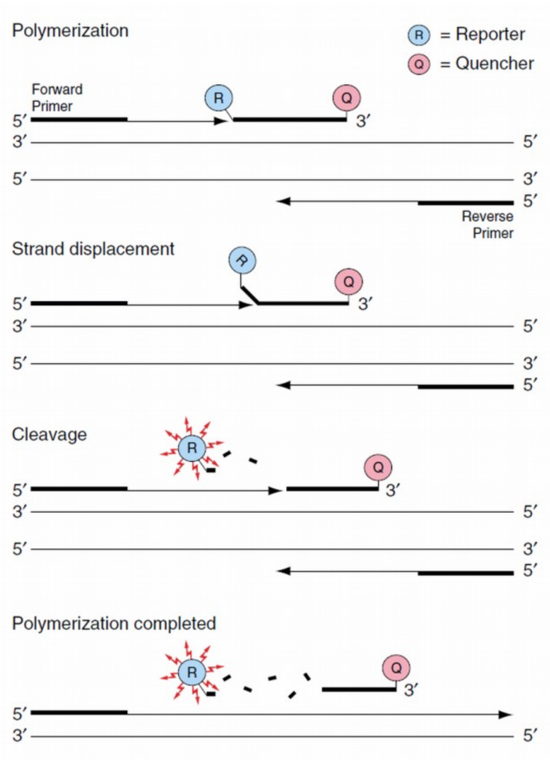

Fig. 12: Fluorescence during PCR (96)

During the PCR reaction AmpliTaq Gold® DNA Polymerase cleaved the TaqMan® probe (Fig. 12). The latter consisted of an oligonucleotide with a 5’ fluorescent reporter dye and a 3’ quencher dye. The TaqMan® probe hybridized to the complementary target sequence and annealed between the forward and reverse primer. Only under this circumstance AmpliTaq Gold® DNA Polymerase cleaved it which separated the two dyes. This leaded to increased fluorescence of the reporter dye which could be detected. (96)

The specific PCR amplification curve showed this accumulation of fluorescence emission at each reaction cycle (Fig. 13). It consisted of four phases. First comes the linear ground phase (usually the first 10-15 cycles) in which the PCR was starting, the fluorescence emission was still below the background fluorescence and a baseline was calculated. In the second phase, the early exponential phase, the so called cycle threshold (C_t) appeared. It was the point in time when the target amplification was first detected and thus fluorescence intensity was greater than the background fluorescence. This was used for experimental calculations. The third phase was the log-linear or exponential phase, where the amplification happened in optimal conditions and the PCR products doubled each cycle. As a fourth step was the plateau stage where the reaction components eventually limited proper amplification. (99)

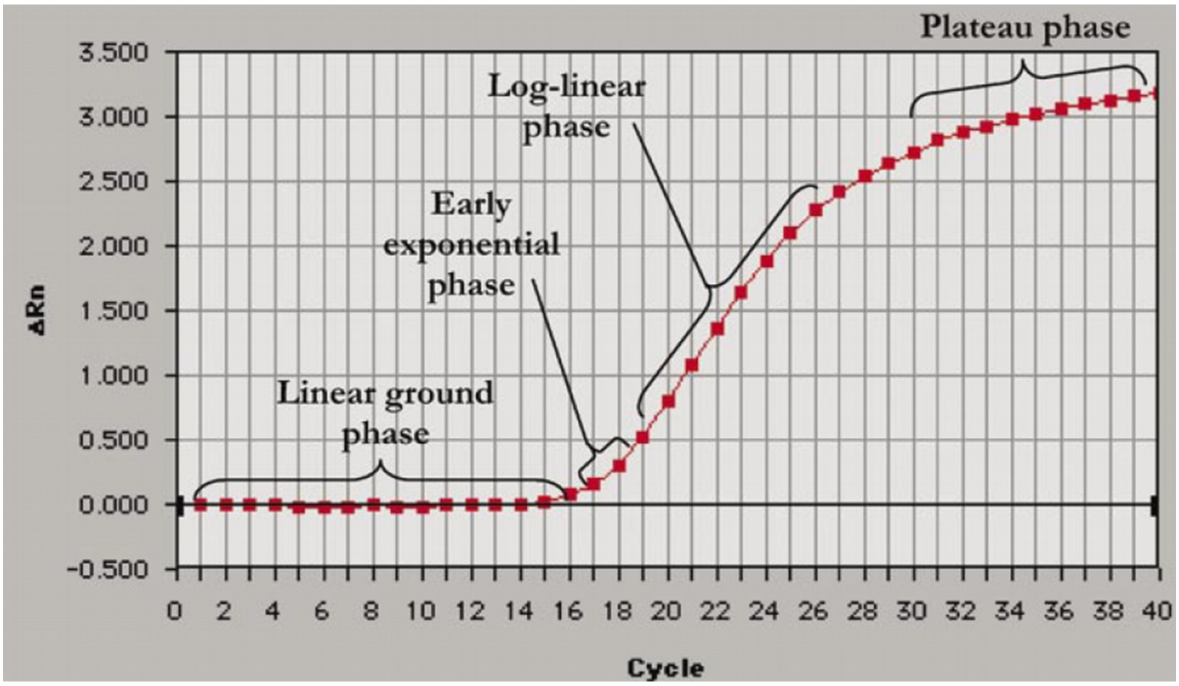

Fig. 13: amplification phases in real time PCR (99)

There is a linear relationship between C_t and amount of total RNA or cDNA, thus the concentration of the samples can be established through their C_t values, given that standards and samples have similar amplification efficiencies. (99)

To analyze our data we used relative quantification with the Standard curve method. For each experimental sample the amount of the target and the endogenous control was determined from their standard curves. Next, the target amount was divided by the endogenous control amount. This resulted in a normalized target value. The means of the double samples were calculated. As a last step changes in gene expression of cells treated with siRNA compared to untreated cells were determined. (101)

3.4. SDS PAGE & Western Blot

To investigate the effects of siRNA directed against *BCS1L* moreover on protein level SDS PAGE and Western Blot were performed.

Cell lysate preparation

To be able to run samples on a gel the cells need to be lysed first so the proteins of interest are released. They are solubilized and can migrate individually through a seperating gel, (102) according to their electrophoretic mobility. (103)
Therefore, HepG2 cells were harvested and washed with PBS, then 50µl of freshly prepared and ice cold lysis buffer was added to each sample. Lysis buffer was prepared of 475µl of an already made stock buffer (10ml including 1.9ml 2M Tris pH 6.8, 5ml Glycerol, 1g SDS and H_2O), 25µl β-mercaptoethanol, 50µl bromphenolblue 0.4% and 1100µl complete protease inhibitor mini +EDTA.
Tris is short for tris[hydroxymethyl]aminomethane ($C_4H_{11}NO_3$, 2-Amino-2-hydroxymethyl-propane-1,3-diol) a common buffering agent. SDS sodium dodecyl sulphate is an anionic detergent effective in both acidic and alkaline solutions. It denatures proteins and dissociates multimeric structures into their subunits. The secondary and non–disulfide–linked tertiary structures are denaturated. SDS further applies a negative charge to each protein in proportion to its mass. Without SDS proteins with similar molecular weights would not migrate the same way within the gel due to differences in mass charge ratio. (103)

As soon as the lysisi buffer is added proteolysis, dephosphorylation and denaturation start. To slow down these events samples needed to be kept on ice and inhibitors are added including ECTA short for ethylene-diamine-tetraacetic acid inhibits Metalloproteases that require Mg^{++} and Mn^{++}. (102)
The samples were sonicated at amplitude of 60 for 10 seconds, to disrupt the cells by disposing them to high-frequency sound waves.

SDS PAGE

Then we proceeded to SDS PAGE (sodium dodecylsulfate polyacrylamide gel electrophoresis). A 13,6% separating gel was made of 3.99ml H_2O, 2.5ml 1.5M Tris ph 8.8, 0.1ml 10% SDS, 3.4ml Acrylamid 40%, 50µl 10% APS (Ammoniumpersulfat) and 5µl Temed (Tetramethylethylenediamine). The gel was gently poured into a gel caster, H_2O was added on top and the gel was allowed to polymerize which is initiated by APS and Temed for at least 30 minutes. Then, a 4% stacking gel was prepared of 3.66ml H_2O, 1.25ml 1.5M Tris pH 6.8, 50µl 10% SDS, 487.5µl Acrylamid 40%, 25µl 10% APS and 5µl Temed. When the separating gel was polymerized, the H_2O was removed and the caster was filled up with stacking gel. A comb was added to create wells for loading. The stacking gel was also given 30 minutes time for polymerization. These gels are neutral, hydrophilic, three-dimensional networks of long hydrocarbons crosslinked by methylene groups. (102) Molecules are separated by pore sizes within the gels. These pores are formed determined by the total amount of acrylamide present (%T) and the amount of cross-linker (%C). (102)
Electrode buffer (SDS buffer) was made of 3g Tris base, 14.4g Glycine, 1g SDS and 1l H_2O. The electrophoresis apparatus was set up including the polymerized gel and the electrode buffer poured into the chamber. The proteinlysate was heated to 99°C so H_2O evaporates.
The wells were filled with 10-20µl of the proteinlysate samples. Additionally, 5µl of PageRuler™ prestained protein ladder (purchased from Fermentas®) was added.
For the first 15 minutes 100 voltages was applied then increased to 200 voltages. The negatively charged proteins migrated across the gel towards the anode. Their speed is determined by the mass to charge ratio which is related to the size of the protein. (103)

After about 35 to 45 minutes the migration front of the PageRuler™ reached the bottom of the gel and the electrophoresis experiment was halted.

Electroblotting

The next step was electroblotting to transfer the proteins to a membrane which "blots" the proteins from the gel. Since the proteins have an electrical charge from the SDS bound to them an electrical field is used to make them travel to the membrane. (102)

The membrane used was PVDF (polyvinylidene fluoride) which need to be activated with methanol for 15 seconds. Subsequently the activated membrane was put in transfer buffer. The transfer buffer was prepared of 5.82g 48mM Tris base, 2.93g 39mM Glycine, 200ml 20% ethanol, 1.88ml 1.3mM 20% SDS and filled up to 1l with distilled H_2O.

In the blotting apparatus first Whatman™ filter paper was fixed, then the activated membrane was added, afterwards the gel and at last another Whatman™ filter paper was placed on top. The proteins moved again towards the positively charged pole in about 2 hours.

Binding Antibodies

After the blotting procedure antibodies were bound to the membrane. First, the membrane needed to be blocked though to prevent any non-specific background binding of the primary or secondary antibodies. (102) The blocking buffer contained PBST (Phosphate-buffered saline Tween) and 5% "non fat dry milk". The membrane was blocked either at room temperature for one hour or at 4°C over night.

The primary antibodies selectively binding to BCS1L and RISP respectively were diluted in PBST 1:1000 and added onto the membrane, which was constantly swayed to obtain an equal distribution of the antibodies and incubated for two hours. Then the membrane was washed 3 times with PBST each 3 minutes.

Afterwards the secondary antibody, a polyclonal goat anti-mouse conjugated to HRP (horse radish peroxidase) was diluted in PBST 1:2500, added onto the membrane, incubated and again swayed for two hours. HRP is a histochemical

tracer used to amplify a weak signal and increase detectability of the target protein.
The membrane was washed in 100ml PBST and 1.17g 0.2M NaCl two times each 10 minutes and washed in only PBST for another 10 minutes.
In the dark room the membrane was incubated with Amersham ECL™ (Enhanced Chemiluminescence), exposed for 3 minutes to Amersham Hyperfilm ECL™ and developed.
ECL is a generic detection system. HRP catalyzes the oxidation of luminol in the presence of peroxide leading to the formation of luminol radicals. These radicals decay through an intermediate compound (3-aminophthalate). During the decay light is emitted at a wavelength of 428 nm and enhanced over 1000 fold. Thus, it can be captured on blue-light sensitive X-ray films and developed on hard copies for analyzes. (104)
Besides the possibility to develop X-ray films multiple times, also the membrane can be recycled. Therefore, it needed to be incubated with stripping buffer to detach the antibodies. After a washing procedure it was ready to be used again for blocking and incubation with new different antibodies.

3.5. Blue Native PAGE & Western Blot

In contrast to SDS PAGE were proteins are denatured, Blue Native PAGE (Blue Native polyacrylamide gel electrophoresis, BNP) gives the opportunity to examine proteins within their protein complex structures. It is utilized to determine native protein masses, oligomeric states and identify physiological protein-protein interactions. (105)

Mitochondrial preparation

First mitochondrial preparation was preformed. HepG2 cells were harvested as usual and resuspended in 1ml PBS. All of the following steps were carried out on ice. The cells were sonicated for 15 seconds at amplitude 60, vortexed and diluted in distilled H_2O 1:10. Via NanoDrop® the protein concentration was measured with absorbance at 280nm. Cells were centrifuged at 2500 rpm at 4°C for 5 minutes. Thereafter the cells were resuspended in PBS to a final concentration of 5mg/ml. 0.05% Digitonin was added and incubated on ice. Digitonin is a non-ionic detergent used for the solubilisation of biological membranes. It is one of the mildest detergents. (105)

PBS was added to a final volume of 2ml. The suspension was centrifuged at 10.000g (9150 rpm) for 10 minutes at 4°C and furthermore the cell pellet was resuspended in MB2 buffer. Subsequently 1/10 of the MB2 volume was added of Lauryl maltoside LM 10% (n-Dodecyl-β-D-maltoside), which gave a final LM concentration of 1%. LM is a non-ionic detergent. The cell suspension was incubated on ice for 15 minutes. Again centrifugation was done at 20.000g at 4°C for 20 minutes.

The supernatant was transferred to a new tube and protein concentration was measured. Finally the dye Coomassie Brilliant blue G-250 ½ of LM volume was added. A synonyme for Coomassie blue G-250 dye is Serva Blue G (SBG). It is an anionic dye which is soluble in H_2O; however, it can bind to membrane proteins due to its hydrophobic properties.

Aliquots were made of the samples and frozen at -80°C and gel electrophoresis was preformed, respectively.

Gel electrophoresis

NativePAGE™ Novex® 4-16% Bis-Tris Gel 1.0 mm was purchased from Invitrogen®. It is a pre-cast polyacrylamide mini gel system with near neutral pH which provides maximum stability for proteins and gel matrix.

The blue cathode buffer contained 15mM Bis-Tris, 50mM Tricine ph 7.0 and 0.02% Comassie dye and the anode buffer 50mM Bis-Tris pH 7.0. We were running the gel at 12 miliAmpere. After the blue running front was about two-thirds along the gel, we removed the blue cathode buffer and added cathode buffer instead which contained 15mM Bis-Tris and 50mM Tricine ph 7.0. This was done for better detection of faint protein bands and to improve blotting so Comassie blue did not compete with protein binding to the membrane. Electrophoresis was stopped after 2 to 4 hours.

Proteins which bind a large number of Coomassie dye molecules underwent a charge shift. Therefore even basic proteins migrated to the anode at pH 7.5 during electrophoresis. Proteins are not separated based on their mass to charge ratio, but to size in acrylamide gradient gels. The pore size decrases throughout the gel and proteins have to stop when they reach their size dependent specific pore-size limit. (105)

When Coomassie dye occupies membrane protein surfaces they lost their hydrophobic character and were converted into H_2O-soluble proteins. Thus, no detergent was needed and the risk of denaturation during BNP was minimized. (105)

Electroblotting was performed semidry. Incubation was done with mitochondrial antibodies purchased from MitoSciences®, secondary antibody was goat anti-mouse/HRP purchased from Dako.

3.6. Oxygen consumption

To analyze the efficacy of the respiratory chain we used Oroboros® Oxygraph-2k (Fig. 14) for high resolution respirometry. The Oxygraph-2k is the base unit of the MultiSensor Mitochondrial Physiology Network Analyzer (O2k-MiPNetAnalyzer). The main function of it is high resolution analysis of O_2 concentration and flux. (107)

Fig. 14: Oroboros® Oxygraph-2k (106)

The machine contained two glass chambers in a copper block with titration-injection openings. Polarographic O_2 sensor (POS) is located within the chambers. It consists of a gold cathode and a silver-silver anode connected by a potassium chloride (KCl) electrolyte solution enclosed by an O_2-permeable membrane. Magnets generate an electromagnetic field in order to rotate the PEEK (polyetheretherketone) stirrer bars inside the chambers. The chambers are connected to the Software DatLab which charts the O_2 concentration and flux measured by POS. (107) Within the diagram the blue line

indicated the O_2 consumption and the red one the O_2 flux. (108) The two chambers can be run at the same time to compare respiratory chain activities of HepG2 cells treated with *BCS1L* siRNA versus untreated HepG2 cells. Per chamber we used 1 Million HepG2 cells in 2.15ml GIBCO™ RPMI Medium 1640.
Beforehand experiments started an O_2 calibration at air saturation with distilled H_2O was necessary. (107) It was crucial to work in a clean and dry environment. Mitochondria are very sensitive to contamination.
The cell suspensions were added to the chambers and were securely sealed with the stopper without causing any air bubbles. First a stable respiratory baseline was established including endogenous substrates with P_i in the medium but no adenylates. (109) Following our protocol mitochondria and respiratory chain, respectively were inhibited and stimulated by adding different kinds of toxins. First, 2µl Oligomycin (Omy) 5mg/ml was added to inhibit complex V, therefore there was respiration without active ATP synthase. (109) This followed a slow titration of 0.1 to 0.2µl FCCP 20mM or 2mM (Carbonyl cyanide p-(trifluoromethoxy) phenylhydrazone) to stimulate mitochondria. FCCP is a mitochondrial uncoupler acting as a protenophore which dissipates the mitochondrial membrane potential. Thus it causes the maximum activation of the electron transport system. (110) After this step 1µl Rotenone (Rot) 2mM was added. This toxin inhibits complex I, (109) the substrates malate and glutamate for NADH are decreased. As a last step we added Antimycin A (Ama), which inhibits complex III by binding to the Q_i site. (33) In this inhibited state (Rot and Ama) mitochondria are not working properly and the residual O_2 consumption is due to cellular, nonmitochondrial O_2 consumption. (110)
After a successful run the machine was stopped and 1.5ml saved for a Cardiolipin assay which is part of the mitochondrial membrane to be able to quantize the analysed mitochondria. Then the chambers were washed with H_2O and ethanol thoroughly. In the end we preformed analyzes and calculations of the experiments.
Additionally, experiments with GRACILE mouse livers were performed. Therefore mitochondria needed to be isolated from the tissue first. 5mg/ml mitochondria concentration were then added to the chambers and analyzes were carried out similar to the protocol for HepG2 cells.

3.7. Immunofluorescence

We also conducted Immunofluorescence experiments to be able to estimate the amount of mitochondria in HepG2 cells. Therefore we used antibodies against pyruvate dehydrogenase subunit E1 (PDH E1) and complex III subunit Core1.
Mitochondrial PDH catalyzes the formation of acetyl-CoA and CO_2 from pyruvate.
Additionally, we used antibodies against Immunglobulin G1 (IgG1) and normal goat serum without any antibodies (NGS) as negative controls.
After the HepG2 cells were harvested and counted, 25.000 cells per specimen were suspended in 300µl PBS. Glass slides and filters were placed in the cytospin, the filters facing the centre of the cytospin to absorb the excess fluids from the cells. Then the cell suspensions were added into the specific wells and centrifuged for 5 minutes at 400xg.
Afterwards the filters were removed from the slides; the cells were marked in a ring with a hydrophobic barrier pen and fixed with 4% Formaldehyd in PBS for 15 minutes. The slides were washed with PBS three times. For permeabilization the cells were incubated with 0,1% Triton X 100 a non-ionic detergent used to solubilize proteins in PBS at room temperature for 15 minutes. Again a three times washing procedure was performed. The next step was blocking with 10% goat serum in 0,1% Triton X 100/PBS for one hour at room temperature.
Subsequently, the primary antibodies (purchased from MitoSciences®) were added. For each antibody we used one slide with treated and untreated cells. The concentrations of the antibodies used were PDH E1 1mg/ml, Core1 100µg/ml, and IgG1 100µg/ml. The slides were incubated over night at 4°C.
The next day the slides were washed with PBS 3 times for 3 minutes. In the dark room the secondary fluorescence antibody anti-IgG1-FITC (fluorescein isothiocyanate) 2µg/ml, which recognizes the primary antibodies, diluted in 10% goat serum/0,1% Triton X 100/PBS was incubated for 2 hours at room temperature. Afterwards it was washed again 3 times for 3 minutes in PBS.
As a final step anti-fade mounting medium was dropped slowly onto the slides and the slides were covered with a thin glass piece. The following day it was sealed with nail polish.
The slides were analysed and photographed with a fluorescence microscope.

4. Results

4.1. Gene expression of *BCS1L* and *RISP*

Gene expression of *BCS1L* and *RISP*, respectively, were efficiently downregulated by RNAi.

We were able to show knockdown of *BCS1L* mRNA in several 6 day experiments. (Fig. 15) After one transfection and 2 days the mean remaining expression of *BCS1L* mRNA was still 42,25% of the basal expression of *BCS1L* mRNA of untreated cells. After two transfections and 4 days 20% and after the third transfection and 6 days only 17,08% (SD 5,6) *BCS1L* mRNA expression was detected. In general we observed a decrease in expression of *BCS1L* mRNA after each transfection. Our best result in one experiment was a 90% downregulation of *BCS1L* mRNA, hence 10% remaining basal expression.

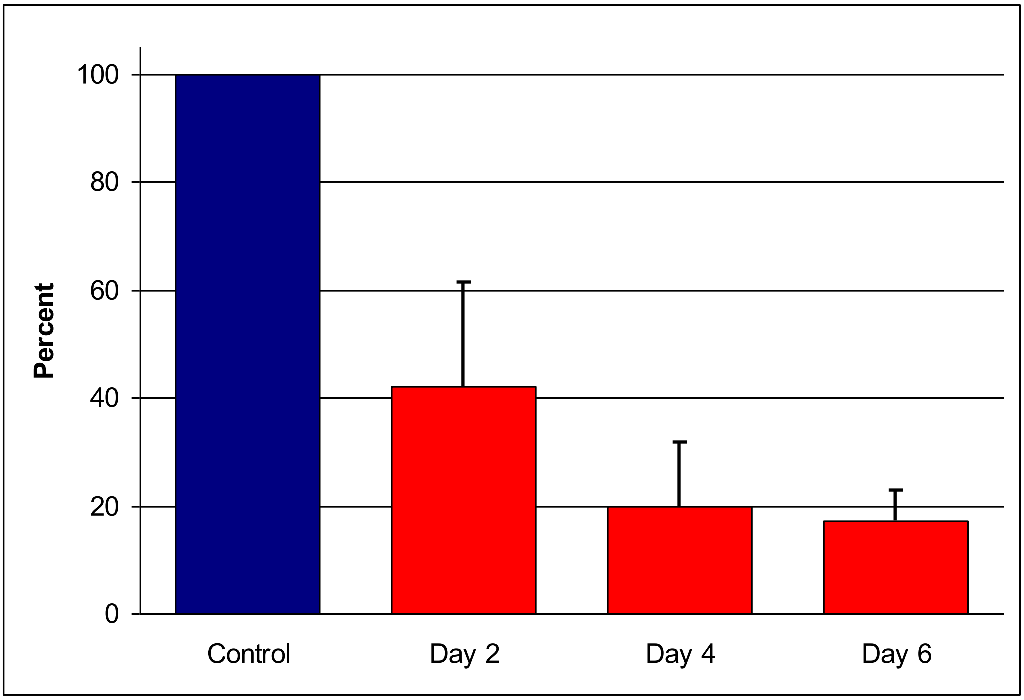

Fig. 15: real time PCR
downregulation of *BCS1L* mRNA compared to untreated control cells after 6 days

The *RISP* siRNA experiments are still in the optimization process. For now we were able to detect a trend that for good downregulation we needed fewer cells than in *BCS1L* siRNA experiments. Additionally, it seems to be more efficient to use shorter time intervals between new transfections. After one day we achieved 7,08% remaining *RISP* expression compared to untreated cells and after two days with all other parameters kept in the same conditions we detected a rise to 17,75% of the basal expression. (Fig. 16)

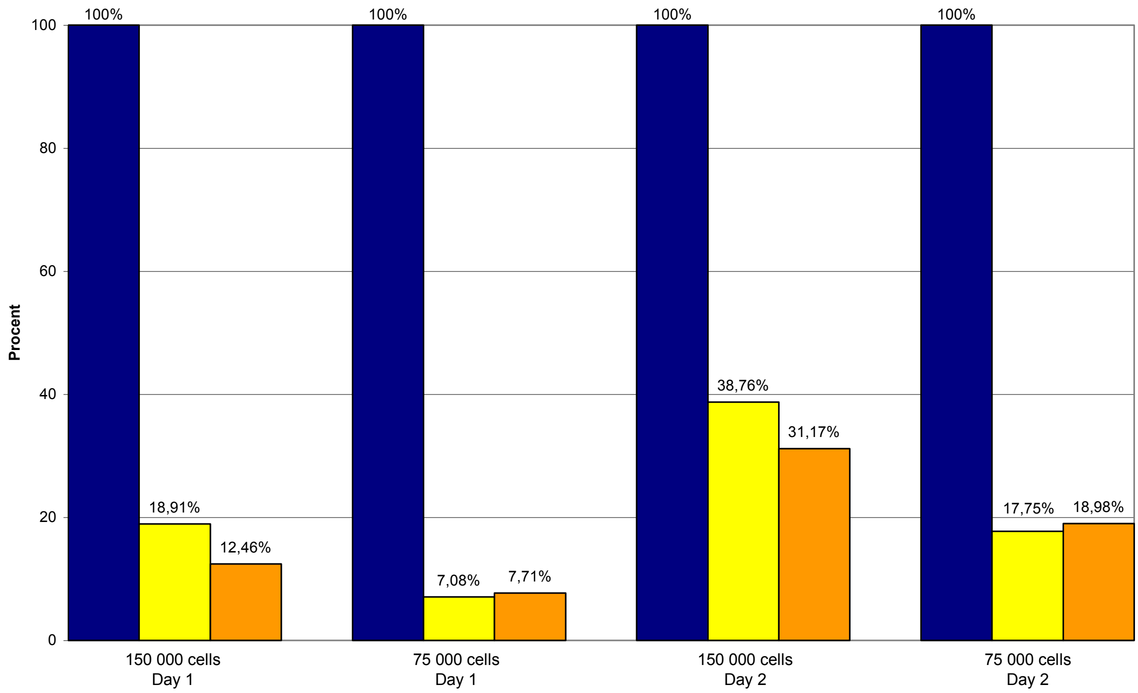

Fig. 16: real time PCR
downregulation of *RISP* mRNA compared to control cells
■ control cells, 6µl HiPerFect, ■ 5nM siRNA, 6µl HiPerFect, ■ 10nM siRNA, 6µl HiPerFect

The best downregultation was achieved at 5 nM siRNA concentration for both *BCS1L* and *RISP* siRNA.

We also analyzed other mRNAs via real time PCR specifically *HIF1α*, *Hepcidin, Ferroportin, Ferritin*, and *TfrR2*, however, could never detect any significant down- or upregulation as a result of *BCS1L* mRNA downregultaion.

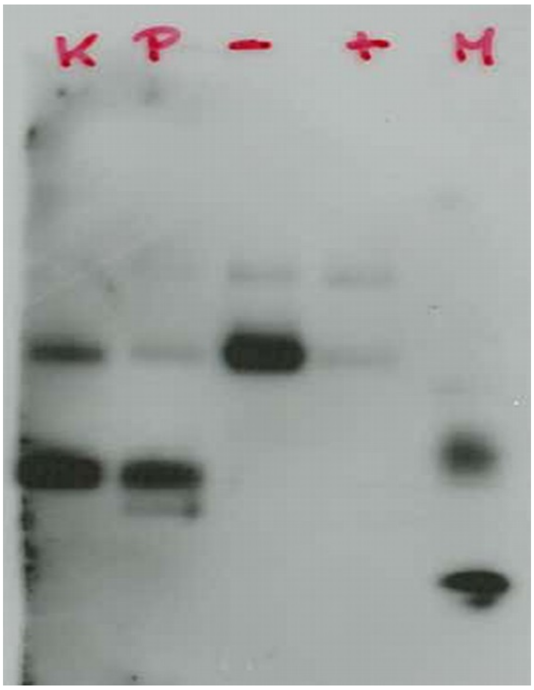

Fig. 17: Western-Blot against BCS1L

K: control
P: patient
-: untreated HepG2 cells
+: BCS1L siRNA treated HepG2 cells
M: marker

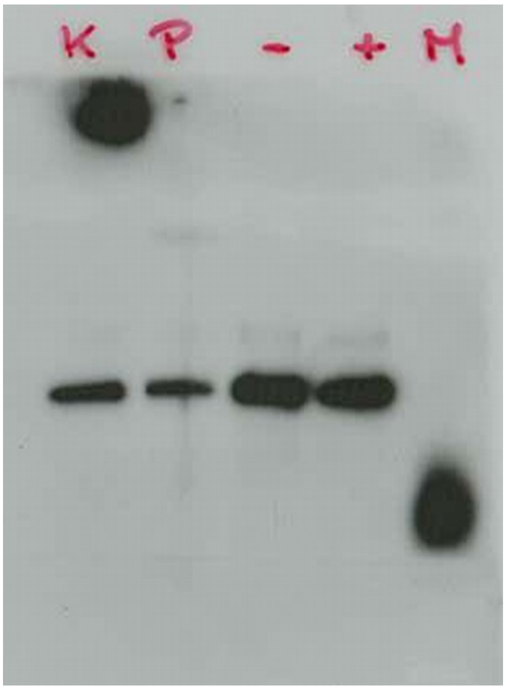

Fig. 18: Western-Blot against RISP

K: control
P: patient
-: untreated HepG2 cells
+: BCS1L siRNA treated HepG2 cells
M: marker

For investigations of the *BCS1L* siRNA experiments at protein levels Western Blot with antibodies against BCS1L and RISP respectively was preformed. Additionally, samples from GRACILE patients and a patient control were added.

BCS1L protein showed a significant decrease in HepG2 cells and the GRACILE patient in comparison to untreated cells and the patient control. BCS1L was fairly detectable. (Fig. 17)

RISP showed an equal overall cellular expression. (Fig. 18)

4.2. Mitochondrial effects of BCS1L downregulation

4.2.1. Complex III formation

In order to detect the effect of *BCS1L* siRNA knockdown on RISP incorporation in complex III on mitochondrial level we performed BNP.
The downregulation of BCS1L itself can be observed from day 2 after transfection, although a little amount of protein is left. However, after 4 and 6 days (as well as 7 days as a control from a previous experiment) basically no protein is left to detect. (Fig. 19)
On the contrary, the incorporation of RISP into complex III of the respiratory chain (Fig. 20) is remaining nearly normal (91,8%) compared to untreated samples. (Amount of proteins calculated and comparison to controls is shown in Fig. 21). RISP consists to be incorporated into complex III as well on day 4 with 79% suggesting/indicating a longer half-life of the protein. Although a significant loss of RISP in complex III can be seen on day 6 (12,3%) respectively day 7 (7,2%).
Antibodies against complex IV and complex II were used as loading controls.

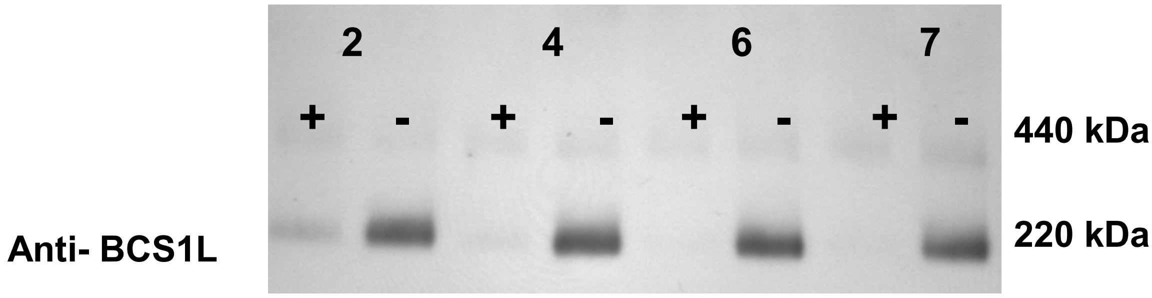

Fig. 19: Blue Native PAGE: Anti-BCS1L

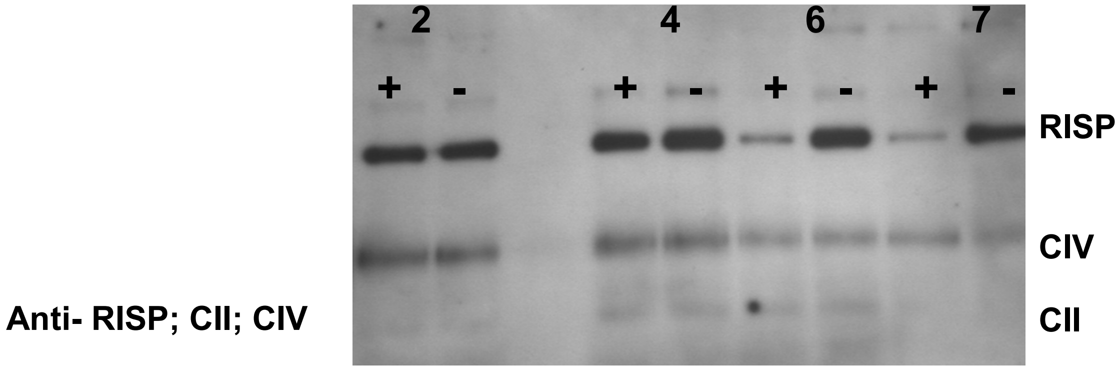

Fig. 20: Blue Native PAGE: Anti-RISP

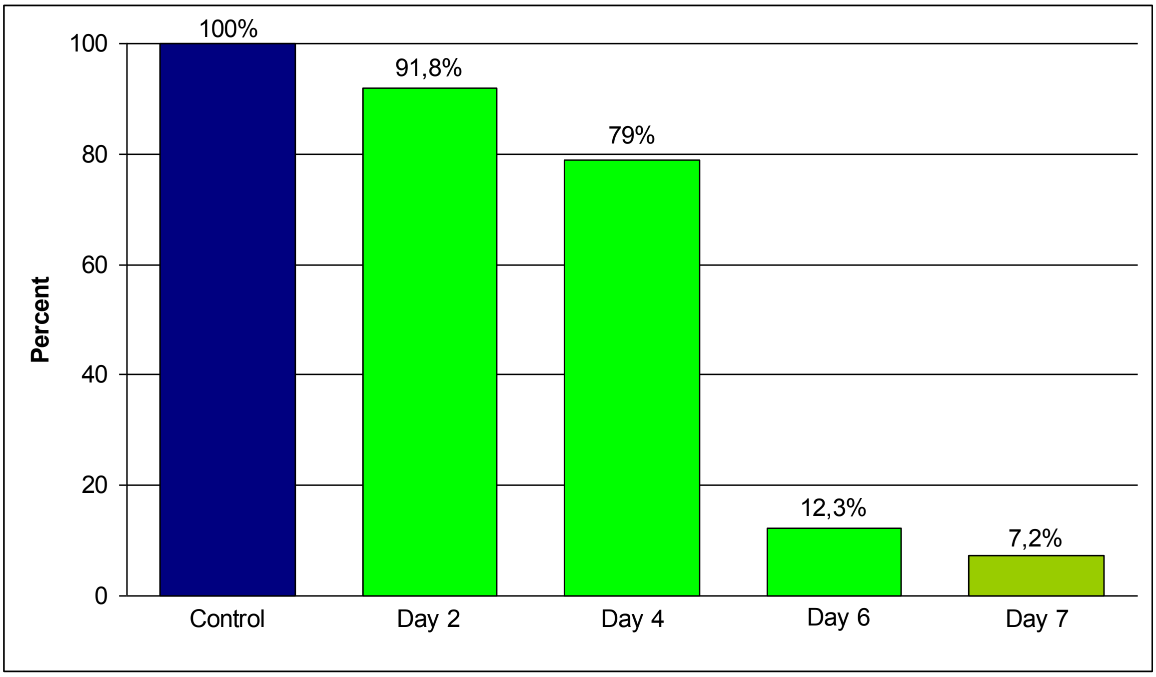

Fig. 21: Blue Native PAGE
Amount of remaining RISP protein after transfection with *BCS1L* siRNA

4.2.2. Mitochondrial respiration

We performed high resolution respirometry analysis (Oroboros O2k Oxygraph) with HepG2 cells transfected 3 times over 6 days. Approximately one million of cells where added to each chamber. Both started with a basal O_2 flow of 30. Adding the different toxins and inhibitors leads to a characteristic curve. We were never able to observe any significant differences in treated and untreated cells. One example is illustrated here. (Fig. 22 and Fig. 23)

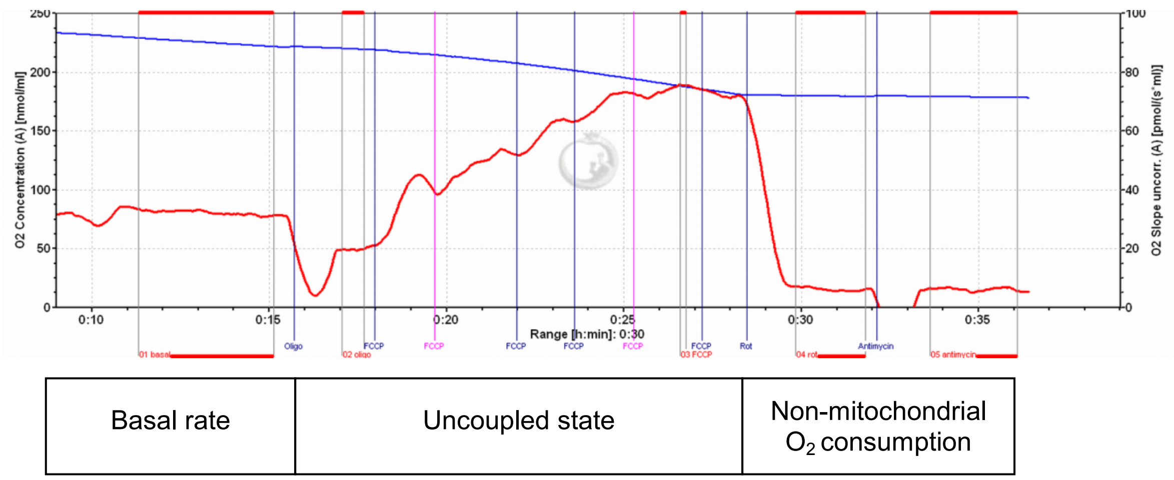

Fig. 22: Oxoboros 2Ok Oxygraph
HepG2 cells treated with siRNA (3 transfections/6 days)

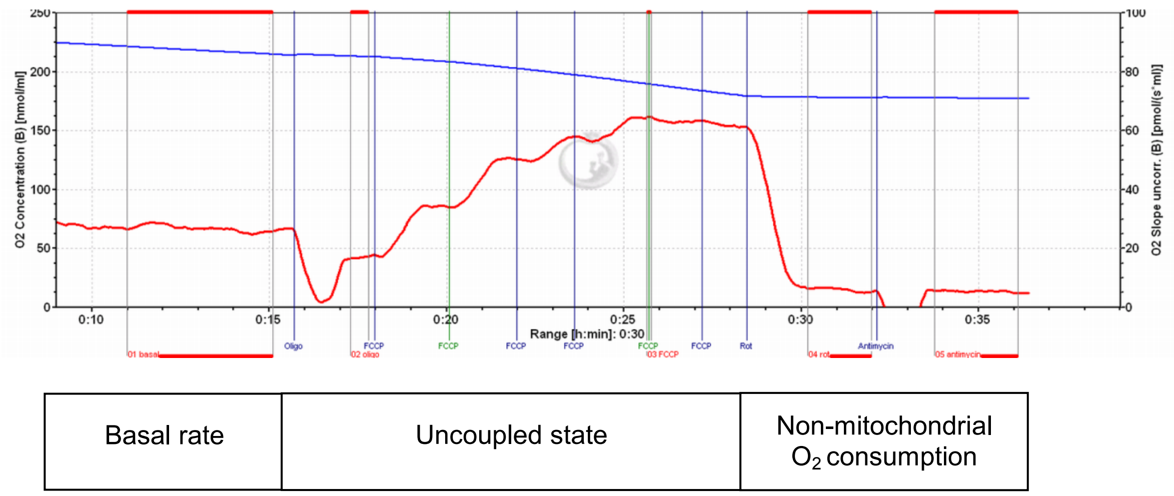

Fig. 23: Oxoboros 2Ok Oxygraph
untreated HepG2 cells

4.3. Cellular content of mitochondria

Immunofluorescence was performed to estimate the amount of mitochondria in HepG2 cells. Antibodies against PDH E1 and Core1 were used (Fig. 24 and Fig. 25).

We were not able to determine any cellular changes within transfected cells in control to untreated cells, including no increase in amount of mitochondria. In both siRNA treated and untreated HepG2 cells the number of mitochondria appears to be approximately the same.

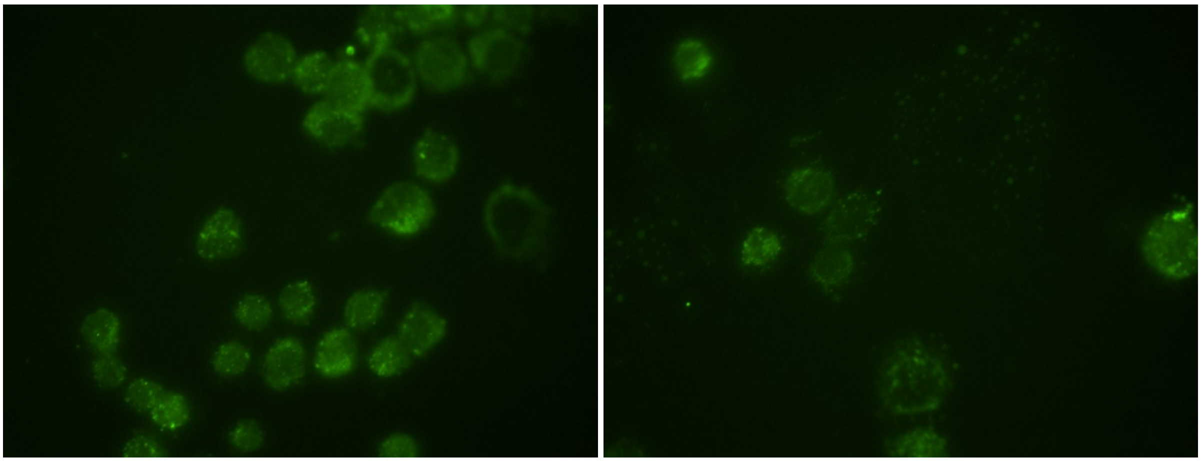

siRNA treated HepG2 cells　　　　untreated HepG2 cells

Fig. 24: Immunofluorescence: antibodies against pyruvate dehydrogenase subunit E1 (PDH E1)

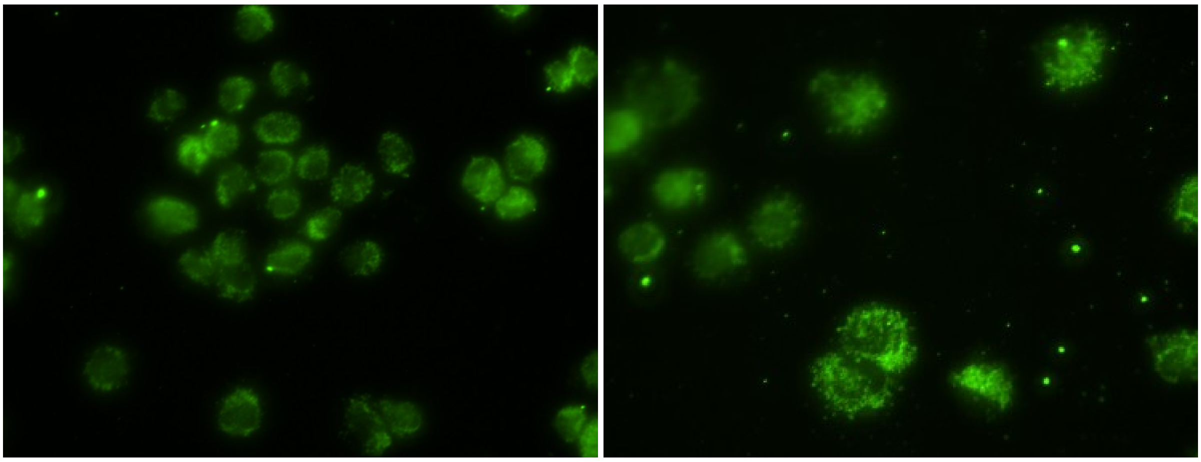

siRNA treated HepG2 cells　　　　untreated HepG2 cells

Fig. 25: Immunofluorescence: antibodies against complex III subunit Core1

5. Discussion

The GRACILE syndrome caused by a homozygous point mutation in the *BCS1L* gene (32) is characterized by growth retardation, aminoaciduria, cholestasis, iron overload, lactic acidosis and early death. (50) Other mutations in *BCS1L* result in very different phenotypes. Complex III deficiencies are caused by various mutations in *BCS1L* leading to encephalopathy alone or with visceral involvement. (37) The Bjönstad syndrome is associated with sensorineural hearing loss and pili torti but otherwise compatible with normal adult life.
BCS1L protein acts as a chaperone for the proper incorporation of RISP into complex III of the respiratory chain. However, BCS1L is likely to have other so far unknown functions. It might be involved in iron metabolism, production of ROS, maintenance of mitochondrial morphology and development of neuronal structures. (32) (44) (45) (46)

The focus of our experiments was to create a human hepatocarcinoma cell model (HepG2 cells) missing BCS1L protein. HepG2 cells were chosen since liver is the target organ of GRACILE syndrome. Carcinoma cell lines serve as easy to study *in vitro* models to investigate effects of the lack of proteins on cellular level.
We hypothesized siRNAs can be used to be able to study the loss of BCS1L function within HepG2 cells. The aims of the study were to efficiently downregulate BCS1L and secondly to assess the effects of this downregulation on the mitochondrial respiratory chain function and the cells iron metabolism.
Conducting our siRNA experiments we were able to sufficiently downregulate *BCS1L* mRNA and protein, respectively. On protein level when performing SDS PAGE and Western Blot BCS1L showed a significant decrease whereas cellular RISP amount was normal as expected. Following, the missing incorporation of RISP into complex III was then demonstrated with BNP and Western Blot. This confirmed the function of BCS1L as a chaperone for RISP.
Additionally, cells contained an equal amount of mitochondria studied by Immunofluorescence. The immunofluorescence experiments revealed that the cells have been in an unhealthy state. This poor cell condition might have been caused either by unrecognized infection or by the transfections with siRNA.

RNAi is shown to be a useful method in order to study the effects on cells missing a certain protein (76). However, our experiments still need further investigations how the transfections affect the cells. It is important to determine whether the siRNAs itself, the transfection reagent HiPerFect or the repeated transfections instead of only one as in most other protocols influenced the cells viability.

Later on we decided to additionally use siRNA directed against *RISP* to achieve a higher degree of inhibition regarding the incorporation of RISP into complex III. We intended to asses the direct effects of complex III completely lacking RISP on the cells metabolism. These experiments were pilot studies to identify the best experiment conditions and moreover to optimize the amount of cells, siRNAs, transfection reagents, time intervals for each set of experiments. Up until my ongoing experiments we were able to show that for efficient knockdown of *RISP* by siRNA less cells and shorter retransfection intervals are required. Transfections should be repeated on a daily basis.
However, recent experiments with siRNAs directed against *RISP* showed to harm the cells causing cell death or growth inhibiton which is so far still unclear. This appeared in cells with siRNA against RISP, scrambled siRNA and furthermore, cells only treated with HiPerFect when compared to completely untreated HepG2 cells. It is important to carry out more experiments regarding this problem.

BCS1L has a well established role in the respiratory chain but seems to have accessory functions (please compare BCS1L – The mitochondrion, Introduction).
Firstly, we focused on BCS1L's role in the generation of ROS and secondly, in the iron metabolism. The GRACILE syndrome strongly suggests a role of BCS1L in iron metabolism. The patients have hepatic iron overload, associated with abnormal levels of protein involved in iron transfer and storage. (32)
We choose proteins involved in these mechanisms and included real time PCR assays with HIF1α, Hepcidin, Ferroportin, Ferritin and TfrR2. We did not find a constant pattern of up and downregulation of any of those proteins. There seemed to be certain trends, though.

As the cells treated with *BCS1L* siRNA showed normal respiration, we concluded that 10-20% of remaining *BCS1L* expression is sufficient to maintain normal respiration. Under this assumption the impact of BCS1L on the function of complex III might be overestimated. RISP incorporation into complex III was decreased following BCS1L downregulation but not as severely as BCS1L was. The remaining amount of protein might be enough for normal complex III function. Alternatively complex III and especially the Q-cycle may have other alternative pathways they can transfer electrons to and hence bypassing RISP. RISP may be assisted and incorporated into complex III by other chaperones besides BCS1L.

On the contrary the GRACILE syndrome does not show any obvious deficiency in complex III activity as well. Though, the severe lactic acidosis of patients with GRACILE syndrome indicates mitochondrial dysfunction within the respiratory chain (50) and also the defect in the assembly of complex III with improper incorporation of RISP can be shown with BNP. (52) Mitochondria from muscle and liver specimen, from liver, brain, muscle, heart, kidney of urgent autopsies and moreover from patient fibroblasts have been investigated indirectly. (53) Additionally, in liver and muscle homogenates complex III activity has been measured directly. The respiratory chain activity was always within normal range.

Regarding patients with Björnstad snydrome and complex III deficiency show more or less a loss of complex III enzyme activity. (44) The more server clinical phenotypes seem to correlate with the most server deficient complex III activity. (37)

However, the GRACILE syndrome caused by a mutation in *BCS1L* with confirmed lack of BCS1L and RISP incorporation into complex III did not show any respiratory chain defects. The homozygous mutation presents with the most server phenotype resulting in the earliest deaths. The HepG2 cell model showed the same pattern. The cells were lacking BCS1L and RISP protein with missing incorporation but the respiratory chain was within normal range.

In some cases mutations resulting in modified, disfunctioning proteins cause a lot of damage than mutations resulting into completely missing the protein. Dysfunctioning proteins interfere with other processes, are incorporated wrongly, accumulate within the cells and further disturb normal cell function. Proteins which are not synthesized at all or immediately degraded afterwards might not interfere with any physiological processes of the cell. Their functions are compensated or bypassed by other proteins. This paradox effect may be a possible explanation for the GRACILE syndrome as well.

Diseases in which these mechanisms have been found to play a role are Epilepsy and mental retardation limited to females, craniofrontonasal syndrome and Pelizaeus–Merzbacher disease.

Epilepsy and mental retardation limited to females (EFMR) (MIM #300088) is an X-linked genetic disorder displaying an unusual expression pattern. In general females are carriers for diseases caused by mutations on the X-chromosome in the *PCDH19* gene and hemizygous males are affected. However, in EFMR males carrying a mutation on their X-chromosome are spared and clinically unaffected whereas females develop seizures and cognitive impairment. Hemizigous males completely miss PCDH19 protein function which might be compensated by other proteins. In contrast females are mosaics for PCDH19-negative and PCDH19-wild type cells which may scramble cell to cell communication. (111)

Secondly craniofrontonasal syndrome (CFNS) (MIM #304110) is also an X-linked disorder which manifests more severely in females. As EFMR it is described to be induced by cellular interference of wild-type and mutant cell populations. CFNS is characterized by craniofrontonasal dysplasia including severe hypertelorism, depressed nasal bridge and bifid nasal tip, frontal bossing, coronal suture synostosis, corpus callosum agenesis, occasionally cleft lip or palate, asymmetry of the thoracic skeleton, pectoral muscle and breasts, grooved nails and thick wiry hair. (112)

Pelizaeus–Merzbacher disease (PMD) (MIM #312080) is an X-linked recessively inherited leukodystrophy caused by the proteolipid protein (PLP). PLP encodes two of the major myelin proteins of the central nervous system. Small mutations and duplications of PLP result in dysmyelination through oligodendrocte apoptosis. (113) The classic form presents with muscular hypotonia, nystagmus, and motor development delay. The more malignant connatal form is associated with little developmental progress and severe neurologic symptoms. (114) There are some small mutations and also null mutations which do not result in oligodendrocyte apoptosis. Males carrying them present with milder disease. (113)

The underlying pathology of the GRACILE Syndrome could be a similar one to the above described diseases.

6. Importance

The Bcs1 protein has been shown to have an important role for the respiratory chain in yeast. Mutations in the human *BCS1L* gene lead to disorders with various pathologies but its role in the human respiratory chain is less clear than in yeast. Furthermore, the occurrence of massive iron overload in GRACILE patients implicates other unknown functions. Clarifying the involvement of BCS1L in mammalian respiratory chain and iron metabolism would be important for better understanding of mitochondrial disease and iron overload disorders.

Literature

1. Mitochondrial structure. [2010-05-10]; Brooklyn College, City University of New York, Lecture Outline, Biology 4 section FV: Available from: http://academic.brooklyn.cuny.edu/biology/bio4fv/page/mito.htm.
2. Henze K, Martin W. Evolutionary biology: essence of mitochondria. Nature. 2003 Nov 13;426(6963):127-8.
3. McBride HM, Neuspiel M, Wasiak S. Mitochondria: more than just a powerhouse. Curr Biol. 2006 Jul 25;16(14):R551-60.
4. Zeviani M, Di Donato S. Mitochondrial disorders. Brain. 2004 Oct;127(Pt 10):2153-72.
5. DiMauro S, Schon EA. Mitochondrial respiratory-chain diseases. The New England journal of medicine. 2003 Jun 26;348(26):2656-68.
6. Di Donato S. Disorders related to mitochondrial membranes: pathology of the respiratory chain and neurodegeneration. J Inherit Metab Dis. 2000 May;23(3):247-63.
7. Kennady PK, Ormerod MG, Singh S, Pande G. Variation of mitochondrial size during the cell cycle: A multiparameter flow cytometric and microscopic study. Cytometry A. 2004 Dec;62(2):97-108.
8. Yaffe MP. The cutting edge of mitochondrial fusion. Nat Cell Biol. 2003 Jun;5(6):497-9.
9. Anderson S, Bankier AT, Barrell BG, de Bruijn MH, Coulson AR, Drouin J, et al. Sequence and organization of the human mitochondrial genome. Nature. 1981 Apr 9;290(5806):457-65.
10. Yamauchi A. Rate of gene transfer from mitochondria to nucleus: effects of cytoplasmic inheritance system and intensity of intracellular competition. Genetics. 2005 Nov;171(3):1387-96.
11. Truscott KN, Lowth BR, Strack PR, Dougan DA. Diverse functions of mitochondrial AAA+ proteins: protein activation, disaggregation, and degradation. Biochem Cell Biol. 2010 Feb;88(1):97-108.
12. Andersson SG, Karlberg O, Canback B, Kurland CG. On the origin of mitochondria: a genomics perspective. Philos Trans R Soc Lond B Biol Sci. 2003 Jan 29;358(1429):165-77; discussion 77-9.
13. Gray MW, Burger G, Lang BF. Mitochondrial evolution. Science. 1999 Mar 5;283(5407):1476-81.
14. Martin W, Muller M. The hydrogen hypothesis for the first eukaryote. Nature. 1998 Mar 5;392(6671):37-41.
15. NCBI » Bookshelf » Basic Neurochemistry » Inherited and Neurodegenerative Diseases » Diseases of Carbohydrate, Fatty Acid and Mitochondrial Metabolism » Diseases of Carbohydrate and Fatty Acid Metabolism in Muscle 1999 [2010-05-27]; American Society for Neurochemistry: Available from: http://www.ncbi.nlm.nih.gov/bookshelf/br.fcgi?book=bnchm&part=A2967&rendertype=figure&id=A2967
16. Levi S, Rovida E. The role of iron in mitochondrial function. Biochim Biophys Acta. 2009 Jul;1790(7):629-36.
17. Bowtell JL, Marwood S, Bruce M, Constantin-Teodosiu D, Greenhaff PL. Tricarboxylic acid cycle intermediate pool size: functional importance for

oxidative metabolism in exercising human skeletal muscle. Sports Med. 2007;37(12):1071-88.
18. Fernie AR, Carrari F, Sweetlove LJ. Respiratory metabolism: glycolysis, the TCA cycle and mitochondrial electron transport. Curr Opin Plant Biol. 2004 Jun;7(3):254-61.
19. Moczulski D, Majak I, Mamczur D. An overview of beta-oxidation disorders. Postepy Hig Med Dosw (Online). 2009;63:266-77.
20. Ott M, Gogvadze V, Orrenius S, Zhivotovsky B. Mitochondria, oxidative stress and cell death. Apoptosis. 2007 May;12(5):913-22.
21. Rossier MF. T channels and steroid biosynthesis: in search of a link with mitochondria. Cell Calcium. 2006 Aug;40(2):155-64.
22. Luzikov VN. Principles of control over formation of structures responsible for respiratory functions of mitochondria. Biochemistry (Mosc). 2009 Dec;74(13):1443-56.
23. Saraste M. Oxidative phosphorylation at the fin de siecle. Science. 1999 Mar 5;283(5407):1488-93.
24. Cape JL, Bowman MK, Kramer DM. Understanding the cytochrome bc complexes by what they don't do. The Q-cycle at 30. Trends Plant Sci. 2006 Jan;11(1):46-55.
25. Shoubridge EA. Nuclear genetic defects of oxidative phosphorylation. Human molecular genetics. 2001 Oct 1;10(20):2277-84.
26. Roessler MM, King MS, Robinson AJ, Armstrong FA, Harmer J, Hirst J. Direct assignment of EPR spectra to structurally defined iron-sulfur clusters in complex I by double electron-electron resonance. Proceedings of the National Academy of Sciences of the United States of America. 2010 Feb 2;107(5):1930-5.
27. Briere JJ, Favier J, El Ghouzzi V, Djouadi F, Benit P, Gimenez AP, et al. Succinate dehydrogenase deficiency in human. Cell Mol Life Sci. 2005 Oct;62(19-20):2317-24.
28. Diaz F. Cytochrome c oxidase deficiency: patients and animal models. Biochim Biophys Acta. 2010 Jan;1802(1):100-10.
29. Junge W, Sielaff H, Engelbrecht S. Torque generation and elastic power transmission in the rotary F(O)F(1)-ATPase. Nature. 2009 May 21;459(7245):364-70.
30. Elston T, Wang H, Oster G. Energy transduction in ATP synthase. Nature. 1998 Jan 29;391(6666):510-3.
31. Fellman V. Mitochondrial complex III deficiencies in the newborn infant. Drug Discovery Today: Disease Mechanisms. 2006;3(4):421-7.
32. Visapaa I, Fellman V, Vesa J, Dasvarma A, Hutton JL, Kumar V, et al. GRACILE syndrome, a lethal metabolic disorder with iron overload, is caused by a point mutation in BCS1L. American journal of human genetics. 2002 Oct;71(4):863-76.
33. Crofts AR, Holland JT, Victoria D, Kolling DR, Dikanov SA, Gilbreth R, et al. The Q-cycle reviewed: How well does a monomeric mechanism of the bc(1) complex account for the function of a dimeric complex? Biochim Biophys Acta. 2008 Jul-Aug;1777(7-8):1001-19.
34. Nobrega FG, Nobrega MP, Tzagoloff A. BCS1, a novel gene required for the expression of functional Rieske iron-sulfur protein in Saccharomyces cerevisiae. The EMBO journal. 1992 Nov;11(11):3821-9.

35. Cruciat CM, Hell K, Folsch H, Neupert W, Stuart RA. Bcs1p, an AAA-family member, is a chaperone for the assembly of the cytochrome bc(1) complex. The EMBO journal. 1999 Oct 1;18(19):5226-33.
36. Ellis RJ. Molecular chaperones: assisting assembly in addition to folding. Trends Biochem Sci. 2006 Jul;31(7):395-401.
37. Moran M, Marin-Buera L, Gil-Borlado MC, Rivera H, Blazquez A, Seneca S, et al. Cellular pathophysiological consequences of BCS1L mutations in mitochondrial complex III enzyme deficiency. Hum Mutat. 2010 Jun 1.
38. Folsch H, Guiard B, Neupert W, Stuart RA. Internal targeting signal of the BCS1 protein: a novel mechanism of import into mitochondria. The EMBO journal. 1996 Feb 1;15(3):479-87.
39. Stan T, Brix J, Schneider-Mergener J, Pfanner N, Neupert W, Rapaport D. Mitochondrial protein import: recognition of internal import signals of BCS1 by the TOM complex. Mol Cell Biol. 2003 Apr;23(7):2239-50.
40. Nouet C, Truan G, Mathieu L, Dujardin G. Functional analysis of yeast bcs1 mutants highlights the role of Bcs1p-specific amino acids in the AAA domain. J Mol Biol. 2009 May 1;388(2):252-61.
41. Petruzzella V, Tiranti V, Fernandez P, Ianna P, Carrozzo R, Zeviani M. Identification and characterization of human cDNAs specific to BCS1, PET112, SCO1, COX15, and COX11, five genes involved in the formation and function of the mitochondrial respiratory chain. Genomics. 1998 Dec 15;54(3):494-504.
42. de Lonlay P, Valnot I, Barrientos A, Gorbatyuk M, Tzagoloff A, Taanman JW, et al. A mutant mitochondrial respiratory chain assembly protein causes complex III deficiency in patients with tubulopathy, encephalopathy and liver failure. Nature genetics. 2001 Sep;29(1):57-60.
43. Fernandez-Vizarra E, Bugiani M, Goffrini P, Carrara F, Farina L, Procopio E, et al. Impaired complex III assembly associated with BCS1L gene mutations in isolated mitochondrial encephalopathy. Human molecular genetics. 2007 May 15;16(10):1241-52.
44. Hinson JT, Fantin VR, Schonberger J, Breivik N, Siem G, McDonough B, et al. Missense mutations in the BCS1L gene as a cause of the Bjornstad syndrome. The New England journal of medicine. 2007 Feb 22;356(8):809-19.
45. Tamai S, Iida H, Yokota S, Sayano T, Kiguchiya S, Ishihara N, et al. Characterization of the mitochondrial protein LETM1, which maintains the mitochondrial tubular shapes and interacts with the AAA-ATPase BCS1L. J Cell Sci. 2008 Aug 1;121(Pt 15):2588-600.
46. Kotarsky H, Tabasum I, Mannisto S, Heikinheimo M, Hansson S, Fellman V. BCS1L is expressed in critical regions for neural development during ontogenesis in mice. Gene Expr Patterns. 2007 Jan;7(3):266-73.
47. Luft R, Ikkos D, Palmieri G, Ernster L, Afzelius B. A case of severe hypermetabolism of nonthyroid origin with a defect in the maintenance of mitochondrial respiratory control: a correlated clinical, biochemical, and morphological study. J Clin Invest. 1962 Sep;41:1776-804.
48. Chinnery PF, Turnbull DM. Epidemiology and treatment of mitochondrial disorders. Am J Med Genet. 2001 Spring;106(1):94-101.
49. Benit P, Lebon S, Rustin P. Respiratory-chain diseases related to complex III deficiency. Biochim Biophys Acta. 2009 Jan;1793(1):181-5.

50. Fellman V, Rapola J, Pihko H, Varilo T, Raivio KO. Iron-overload disease in infants involving fetal growth retardation, lactic acidosis, liver haemosiderosis, and aminoaciduria. Lancet. 1998 Feb 14;351(9101):490-3.
51. Norio R. Finnish Disease Heritage I: characteristics, causes, background. Human genetics. 2003 May;112(5-6):441-56.
52. Fellman V, Lemmela S, Sajantila A, Pihko H, Jarvela I. Screening of BCS1L mutations in severe neonatal disorders suspicious for mitochondrial cause. Journal of human genetics. 2008;53(6):554-8.
53. Fellman V. The GRACILE syndrome, a neonatal lethal metabolic disorder with iron overload. Blood cells, molecules & diseases. 2002 Nov-Dec;29(3):444-50.
54. Fellman V, Visapaa I, Vujic M, Wennerholm UB, Peltonen L. Antenatal diagnosis of hereditary fetal growth retardation with aminoaciduria, cholestasis, iron overload, and lactic acidosis in the newborn infant. Acta obstetricia et gynecologica Scandinavica. 2002 May;81(5):398-402.
55. Norio R. The Finnish Disease Heritage III: the individual diseases. Human genetics. 2003 May;112(5-6):470-526.
56. Rapola J, Heikkila P, Fellman V. Pathology of lethal fetal growth retardation syndrome with aminoaciduria, iron overload, and lactic acidosis (GRACILE). Pediatric pathology & molecular medicine. 2002 Mar-Apr;21(2):183-93.
57. Visapaa I, Fellman V, Varilo T, Palotie A, Raivio KO, Peltonen L. Assignment of the locus for a new lethal neonatal metabolic syndrome to 2q33-37. American journal of human genetics. 1998 Nov;63(5):1396-403.
58. Khoury M, Beaty T, Cohen B. Fundamentals of Genetic Epidemiology: Oxford University Press; 1993.
59. Visapaa I, Fellman V, Lanyi L, Peltonen L. ABCB6 (MTABC3) excluded as the causative gene for the growth retardation syndrome with aminoaciduria, cholestasis, iron overload, and lactacidosis. Am J Med Genet. 2002 May 1;109(3):202-5.
60. Fellman V, von Bonsdorff L, Parkkinen J. Exogenous apotransferrin and exchange transfusions in hereditary iron overload disease. Pediatrics. 2000 Feb;105(2):398-401.
61. Peltonen L, Jalanko A, Varilo T. Molecular genetics of the Finnish disease heritage. Human molecular genetics. 1999;8(10):1913-23.
62. Sajantila A, Salem AH, Savolainen P, Bauer K, Gierig C, Paabo S. Paternal and maternal DNA lineages reveal a bottleneck in the founding of the Finnish population. Proceedings of the National Academy of Sciences of the United States of America. 1996 Oct 15;93(21):12035-9.
63. Brunelle JK, Bell EL, Quesada NM, Vercauteren K, Tiranti V, Zeviani M, et al. Oxygen sensing requires mitochondrial ROS but not oxidative phosphorylation. Cell Metab. 2005 Jun;1(6):409-14.
64. Klimova T, Chandel NS. Mitochondrial complex III regulates hypoxic activation of HIF. Cell Death Differ. 2008 Apr;15(4):660-6.
65. Pinto JP, Ribeiro S, Pontes H, Thowfeequ S, Tosh D, Carvalho F, et al. Erythropoietin mediates hepcidin expression in hepatocytes through EPOR signaling and regulation of C/EBPalpha. Blood. 2008 Jun 15;111(12):5727-33.
66. Ganz T. Molecular control of iron transport. J Am Soc Nephrol. 2007 Feb;18(2):394-400.

67. De Domenico I, McVey Ward D, Kaplan J. Regulation of iron acquisition and storage: consequences for iron-linked disorders. Nat Rev Mol Cell Biol. 2008 Jan;9(1):72-81.
68. Trinder D, Baker E. Transferrin receptor 2: a new molecule in iron metabolism. Int J Biochem Cell Biol. 2003 Mar;35(3):292-6.
69. Lubianca Neto JF, Lu L, Eavey RD, Flores MA, Caldera RM, Sangwatanaroj S, et al. The Bjornstad syndrome (sensorineural hearing loss and pili torti) disease gene maps to chromosome 2q34-36. American journal of human genetics. 1998 May;62(5):1107-12.
70. Selvaag E. Pili torti and sensorineural hearing loss. A follow-up of Bjornstad's original patients and a review of the literature. Eur J Dermatol. 2000 Mar;10(2):91-7.
71. Richards KA, Mancini AJ. Three members of a family with pili torti and sensorineural hearing loss: the Bjornstad syndrome. Journal of the American Academy of Dermatology. 2002 Feb;46(2):301-3.
72. Ramos-Arroyo MA, Hualde J, Ayechu A, De Meirleir L, Seneca S, Nadal N, et al. Clinical and biochemical spectrum of mitochondrial complex III deficiency caused by mutations in the BCS1L gene. Clin Genet. 2009 Jun;75(6):585-7.
73. Tuppen HA, Fehmi J, Czermin B, Goffrini P, Meloni F, Ferrero I, et al. Long-term survival of neonatal mitochondrial complex III deficiency associated with a novel BCS1L gene mutation. Mol Genet Metab. 2010 Aug;100(4):345-8.
74. Blazquez A, Gil-Borlado MC, Moran M, Verdu A, Cazorla-Calleja MR, Martin MA, et al. Infantile mitochondrial encephalomyopathy with unusual phenotype caused by a novel BCS1L mutation in an isolated complex III-deficient patient. Neuromuscul Disord. 2009 Feb;19(2):143-6.
75. De Meirleir L, Seneca S, Damis E, Sepulchre B, Hoorens A, Gerlo E, et al. Clinical and diagnostic characteristics of complex III deficiency due to mutations in the BCS1L gene. Am J Med Genet A. 2003 Aug 30;121A(2):126-31.
76. Aigner A. Delivery Systems for the Direct Application of siRNAs to Induce RNA Interference (RNAi) In Vivo. Journal of biomedicine & biotechnology. 2006;2006(4):71659.
77. Ding SW, Li H, Lu R, Li F, Li WX. RNA silencing: a conserved antiviral immunity of plants and animals. Virus Res. 2004 Jun 1;102(1):109-15.
78. Tang G. siRNA and miRNA: an insight into RISCs. Trends Biochem Sci. 2005 Feb;30(2):106-14.
79. Jinek M, Doudna JA. A three-dimensional view of the molecular machinery of RNA interference. Nature. 2009 Jan 22;457(7228):405-12.
80. Siomi H, Siomi MC. On the road to reading the RNA-interference code. Nature. 2009 Jan 22;457(7228):396-404.
81. Saxena S, Jonsson ZO, Dutta A. Small RNAs with imperfect match to endogenous mRNA repress translation. Implications for off-target activity of small inhibitory RNA in mammalian cells. J Biol Chem. 2003 Nov 7;278(45):44312-9.
82. Zhang H, Kolb FA, Jaskiewicz L, Westhof E, Filipowicz W. Single processing center models for human Dicer and bacterial RNase III. Cell. 2004 Jul 9;118(1):57-68.
83. Dlakic M. DUF283 domain of Dicer proteins has a double-stranded RNA-binding fold. Bioinformatics (Oxford, England). 2006 Nov 15;22(22):2711-4.

84. Yan KS, Yan S, Farooq A, Han A, Zeng L, Zhou MM. Structure and conserved RNA binding of the PAZ domain. Nature. 2003 Nov 27;426(6965):468-74.
85. Collins RE, Cheng X. Structural domains in RNAi. FEBS Lett. 2005 Oct 31;579(26):5841-9.
86. Sashital DG, Doudna JA. Structural insights into RNA interference. Curr Opin Struct Biol. 2010 Feb;20(1):90-7.
87. Fire A, Xu S, Montgomery MK, Kostas SA, Driver SE, Mello CC. Potent and specific genetic interference by double-stranded RNA in Caenorhabditis elegans. Nature. 1998 Feb 19;391(6669):806-11.
88. HiPerFect Transfection Reagent Handbook. 2008 [2008-09-09]; Qiagen® Sample & Assay Technologies, 5th edition, May 2008: Available from: http://www.qiagen.com/products/transfection/transfectionreagents/hiperfecttransfectionreagent.aspx#Tabs=t2.
89. Knasmuller S, Parzefall W, Sanyal R, Ecker S, Schwab C, Uhl M, et al. Use of metabolically competent human hepatoma cells for the detection of mutagens and antimutagens. Mutation research. 1998 Jun 18;402(1-2):185-202.
90. Javitt NB. Hep G2 cells as a resource for metabolic studies: lipoprotein, cholesterol, and bile acids. Faseb J. 1990 Feb 1;4(2):161-8.
91. Pinti M, Troiano L, Nasi M, Ferraresi R, Dobrucki J, Cossarizza A. Hepatoma HepG2 cells as a model for in vitro studies on mitochondrial toxicity of antiviral drugs: which correlation with the patient? Journal of biological regulators and homeostatic agents. 2003 Apr-Jun;17(2):166-71.
92. RNeasy® Mini Handbook. 2006 [2010-06-20]; Qiagen® Sample & Assay Technologies, 4th edition, April 2006: Available from: http://www.qiagen.com/Products/RnaStabilizationPurification/RNeasySystem/RNeasyMini.aspx?r=1737#Tabs=t2.
93. Gallagher SR, Desjardins PR. Quantitation of DNA and RNA with absorption and fluorescence spectroscopy. Curr Protoc Protein Sci. 2008 May;Appendix 3:Appendix 4K.
94. TaqMan® Fast Universal PCR Master Mix (2×) Protocol. 2005 [2010-06-05]; Applied Biosystems™ by Life Technologies™: Available from: http://www3.appliedbiosystems.com/cms/groups/mcb_support/documents/generaldocuments/cms_041461.pdf.
95. cDNA: Protocol Online - Your lab's reference book. 2010 [2010-07-05]; Available from: http://www.protocol-online.org/prot/Molecular_Biology/RNA/cDNA/index.html.
96. TaqMan® Universal PCR Master Mix Protocol. 2002 [2010-07-05]; Applied Biosystems™ by Life Technologies™: Available from: http://www3.appliedbiosystems.com/cms/groups/mcb_support/documents/generaldocuments/cms_042996.pdf.
97. Random Hexamer Primer. 2010 [2010-07-05]; Fermentas®, Life Science, Part of Thermo Fisher Scientific: Available from: http://www.fermentas.com/en/products/all/nucleotides-primers/other-primers/so142-random-hexamer-primer.
98. Mutliscribe Reverse Transcriptase from Applied Biosystems™. 2010 [2010-07-05]; biocompare® The Buyer's Guide for Life Scientists: Available from: http://www.biocompare.com/ProductDetails/481372/MultiScribe-Reverse-Transcriptase.html.

99. Wong ML, Medrano JF. Real-time PCR for mRNA quantitation. Biotechniques. 2005 Jul;39(1):75-85.
100. TaqMan® Gene Expression Assays - Individual Assays. 2010 [2010-07-25]; Applied Biosystems™ by Life Technologies™:[Available from: https://products.appliedbiosystems.com/ab/en/US/adirect/ab?cmd=catNavigate2&catID=601267.
101. Essentials for Real Time PCR. [2010-04-19]; Applied Biosystems™ by Life Technologies™: Available from: http://www3.appliedbiosystems.com/cms/groups/mcb_marketing/documents/generaldocuments/cms_042485.pdf.
102. Western Blotting - A Beginner's Guide. 2010 [2008-09-20]; abacam®: [Available from: http://www.abcam.com/ps/pdf/protocols/WB-beginner.pdf.
103. SDS-PAGE Gel Electrophoresis. 2008 [2010-06-10]; Molecular Station: Available from: http://www.molecularstation.com/sds-page-gel-electrophoresis/#sds.
104. Durrant I. Enhanced Chemiluminescent Detection of Horseradish Peroxidase Labeled Probes. 1994. p. 147-61.
105. Wittig I, Braun HP, Schagger H. Blue native PAGE. Nat Protoc. 2006;1(1):418-28.
106. Gnaiger E. Top 10 Reasons for OROBOROS INSTRUMENTS, high resolution respirometry, Oxygraph-2k, Mitochondrial Physiology Network 14.10: 1-4 (2010). 2010 [2010-07-23]; Available from: http://www.oroboros.at/fileadmin/user_upload/OROBOROS_Handbook/HRR-10Reasons.pdf.
107. Gnaiger E. The Oxygraph for High-Resolution Respirometry, 1.1.A. Mitochondrial Physiology Network 6.1: 1-19 (2001-2007). 2007 [2010-02-13]; Available from: http://www.oroboros.at/fileadmin/user_upload/O2k_Manual/1.1.A.Oxygraph-Overview.pdf.
108. Gnaiger E. Mitochondrial Pathways through Complexes I+II: Convergent Electron Transport at the Q-Junction and Additive Effect of Substrate Combinations. 2.1.C. Mitochondrial Physiology Network 12.12, in: Gnaiger E, ed (2009) Mitochondrial Pathways and Respiratory Control. 2nd ed, OROBOROS MiPNet Publications, Innsbruck: pp. 21-33. 2009 [2010-02-13]; Available from: www.oroboros.at/index.php?compl-12-convergent.
109. Gnaiger E. MitoPathways: Respiratory States and Coupling Control Ratios. 2.1.E. Mitochondrial Physiology Network 12.15, In: Gnaiger E, ed (2009) Mitochondrial Pathways and Respiratory Control. 2nd ed, OROBOROS MiPNet Publications, Innsbruck: pp. 43-53. 2009 [2010-02-14]; Available from: http://www.oroboros.at/fileadmin/user_upload/OROBOROS_Handbook/2.1.E-RespiratoryStates_MP2.pdf.
110. Gnaiger E. Polarographic oxygen sensors, the oxygraph and high-resolution respirometry to assess mitochondrial function. In: Mitochondrial Dysfunction in Drug-Induced Toxicity (Dykens JA, Will Y, eds) John Wiley: 327-352. 2008 [2010-02-14]; Available from: http://www.oroboros.at/index.php?id=uncoupling&no_cache=1&sword_list[]=FUNCTION.

111. Dibbens LM, Tarpey PS, Hynes K, Bayly MA, Scheffer IE, Smith R, et al. X-linked protocadherin 19 mutations cause female-limited epilepsy and cognitive impairment. Nature genetics. 2008 Jun;40(6):776-81.
112. Wieland I, Makarov R, Reardon W, Tinschert S, Goldenberg A, Thierry P, et al. Dissecting the molecular mechanisms in craniofrontonasal syndrome: differential mRNA expression of mutant EFNB1 and the cellular mosaic. Eur J Hum Genet. 2008 Feb;16(2):184-91.
113. Garbern J, Hobson G. Prenatal diagnosis of Pelizaeus-Merzbacher disease. Prenat Diagn. 2002 Nov;22(11):1033-5.
114. Hanefeld FA, Brockmann K, Pouwels PJ, Wilken B, Frahm J, Dechent P. Quantitative proton MRS of Pelizaeus-Merzbacher disease: evidence of dys- and hypomyelination. Neurology. 2005 Sep 13;65(5):701-6.